Received: 7 January 2022 | Revised: 29 May 2022 | Accepted: 10 June 2022

DOI: 10.1111/1755-0998.13669

MOLECULAR ECOLOGY RESOURCES WILEY

FROM THE COVER

Chromosome-scale genomes reveal genomic consequences of inbreeding in the South China tiger: A comparative study with the Amur tiger

Le Zhang[1] | Tianming Lan[2,3] | Chuyu Lin[4] | Wenyuan Fu[5,6] | Yaohua Yuan[7] | Kaixiong Lin[6] | Haimeng Li[2,8] | Sunil Kumar Sahu[2] | Zhaoyang Liu[9] | Daqing Chen[10] | Qunxiu Liu[7] | Aishan Wang[7] | Xiaohong Wang[11] | Yue Ma[1] | Shizhou Li[12] | Yixin Zhu[2,8] | Xingzhuo Wang[9] | Xiaotong Ren[1] | Haorong Lu[13,14] | Yunting Huang[13] | Jieyao Yu[13] | Boyang Liu[1] | Qing Wang[2,8] | Shaofang Zhang[13] | Xun Xu[14] | Huanming Yang[15,16] | Dan Liu[17] | Huan Liu[2,3] | Yanchun Xu[1,18]

[1]College of Wildlife and Protected Area, Northeast Forestry University, Harbin, China

[2]State Key Laboratory of Agricultural Genomics, Shenzhen, China

[3]BGI Life Science Joint Research Center, Northeast Forestry University, Harbin, China

[4]Shenzhen Zhong Nong Jing Yue Biotech Company Limited, Shenzhen, China

[5]Longyan Geopark Protection and Development Center, Longyan, China

[6]Fujian Meihuashan Institute of South China Tiger Breeding, Longyan, China

[7]Shanghai Zoological Park, Shanghai, China

[8]College of Life Sciences, University of Chinese Academy of Sciences, Beijing, China

[9]Luoyang Zoo in Wangcheng Park, Luoyang, China

[10]Suzhou Shangfangshan Forest Zoo, Suzhou, China

[11]Nanchang Zoo, Nanchang, China

[12]Shaoguan Research Base of South China Tiger, Shaoguan, China

[13]China National GeneBank, Shenzhen, China

[14]Guangdong Provincial Key Laboratory of Genome Read and Write, Shenzhen, China

[15]Guangdong Provincial Academician Workstation of BGI Synthetic Genomics, Shenzhen, China

[16]James D. Watson Institute of Genome Sciences, Hangzhou, China

[17]Heilongjiang Siberian Tiger Park, Harbin, China

[18]National Forestry and Grassland Administration Research Center of Engineering Technology for Wildlife Conservation and Utilization, Harbin, China

Correspondence
Tianming Lan and Huan Liu, State Key Laboratory of Agricultural Genomics, BGI-Shenzhen, Shenzhen, China.
Emails: lantianming@genomics.cn; liuhuan@genomics.cn

Dan Liu, Heilongjiang Siberian Tiger Park, Harbin, China.
Email: liudan_1964@sina.com

Abstract

The South China tiger (*Panthera tigris amoyensis*, SCT) is the most critically endangered subspecies of tiger due to functional extinction in the wild. Inbreeding depression is observed among the captive population descended from six wild ancestors, resulting in high juvenile mortality and low reproduction. We assembled and characterized the first SCT genome and an improved Amur tiger (*P. t. altaica*, AT) genome named

Le Zhang, Tianming Lan, Chuyu Lin, and Wenyuan Fu contributed equally to this work.

Yanchun Xu, College of Wildlife and Protected Area, Northeast Forestry University, Harbin, China.
Email: xu_daniel@163.com

Funding information
Fundamental Research Funds for the Central Universities, Grant/Award Number: 2572020DR10; Guangdong Provincial Key Laboratory of Genome Read and Write, Grant/Award Number: 2017B030301011; Siberian tiger Conservation Project of Forestry and Grassland Department of Heilongjiang Province, China.

Handling Editor: Elin Videvall

AmyTig1.0 and PanTig2.0. The two genomes are the most continuous and comprehensive among any tiger genomes yet reported at the chromosomal level. By using the two genomes and resequencing data of 15 SCT and 13 AT individuals, we investigated the genomic signature of inbreeding depression of the SCT. The results indicated that the effective population size of SCT experienced three phases of decline, ~5.0–1.0 thousand years ago, 100 years ago, and since captive breeding in 1963. We found 43 long runs of homozygosity fragments that were shared by all individuals in the SCT population and covered a total length of 20.63% in the SCT genome. We also detected a large proportion of identical-by-descent segments across the genome in the SCT population, especially on ChrB4. Deleterious nonsynonymous single nucleotide polymorphic sites and loss-of-function mutations were found across genomes with extensive potential influences, despite a proportion of these loads having been purged by inbreeding depression. Our research provides an invaluable resource for the formulation of genetic management policies for the South China tiger such as developing genome-based breeding and genetic rescue strategy.

KEYWORDS
Amur tiger, genetic management, inbreeding depression, South China tiger

1 | INTRODUCTION

The tiger (*Panthera tigris*) is the largest predatory species on the Eurasian continent (Mazák, 1983). It diverged into nine subspecies since the last glacial period (Liu et al., 2018), namely Amur or Siberian tiger (*P. t. altaica*), South China tiger (*P. t. amoyensis*), Indochinese tiger (*P. t. corbetti*), Bengal tiger (*P. t. tigris*), Malayan tiger (*P. t. jacksoni*), Sumatrian tiger (*P. t. sumatrae*), Javan tiger (*P. t. sondaica*), Bali tiger (*P. t. balica*) and Caspian tiger (*P. t. virgata*) (Luo et al., 2004). The populations of all these subspecies have fallen dramatically in the last century as a result of habitat loss, fragmentation and poaching, with the Bali, Javan and Caspian tigers becoming extinct one after the other during the 1940s to 1970s (Seidensticker, 2010). This crisis drew widespread attention, and conservation actions were implemented across the world. The demographic decline was slackened gradually and reversed by 2016 (WWF, 2016).

However, the South China tiger was not included in the restoration programme because it was declared functionally extinct in the wild by the end of the 1990s (Tilson et al., 1996; Tilson et al., 2004). The only representatives remained are the 204-captive descendants (by the end of 2019) (Yuan et al., 2021) of six wild founders. Superficially, the current population number, age structure and sex ratio (Figure S1) are supportive of its sustainability. However, due to the small number of founders and unequal founders' contributions, inbreeding is unavoidable (Xu et al., 2007). This resulted in inbreeding depression that progressively degraded the reproductive capacity of adults and the survival of juveniles despite substantial improvements in captive rearing technology and expertise (Xu et al., 2007; Yuan et al., 2021). In addition, pedigree-based estimation showed that the present population represents 65.23% of the six ancestors' genetic diversity (Yuan et al., 2020), meaning 34.77% has been lost.

Apparently, there is no additional outbred consubspecific individual from any source to join the population, and no pairing scheme within the captive population can avoid further inbreeding. Traditionally, managers have used genealogical records (Tilson et al., 1993), microsatellites and mitochondrial (Zhang et al., 2019) molecular genetic markers to guide the breeding programme of captive tigers. This pairing approach can effectively control the rate of inbreeding accumulation in a short period of time. However, based on the development of a small number of genetic markers this tends to ignore the deleterious effects that accumulate on the genome and the genetic information carried on genes embodied in inbreeding decline. It is clear that inbreeding, together with consequent genetic diversity loss and physiological depression will be exacerbated with time, driving the population toward a genetic dead end.

Research projects on tigers have focused on field population surveys (Ronald Tilson et al., 2004; Huang et al., 2004), habitat selection (Ronald Tilson et al., 1997), tiger pelage colour variations (Luo et al., 2019) and population differentiation (Armstrong et al., 2021; Cho et al., 2013; Liu et al., 2018; Luo et al., 2004), etc., all of which revealed the overall status level of the population. However, the genome-wide inbreeding context of the South China tiger population and how the consequences of inbreeding can be demonstrated at the genome level are largely unknown, which would be necessary and helpful for making sound management recommendations.

In this study, we chose captive Amur tiger individuals as a reference. We investigated whether different tiger subspecies share the same inbreeding cumulative expression patterns on their genomes under the same husbandry conditions. Currently, published

PanTig1.0 (Cho et al., 2013) and Maltig1.0 (Armstrong et al., 2021) tiger genomes were sequenced based on the Illumina sequencing platform. Studies have shown that genomes assembled via short fragments would introduce assembly errors, thus affecting the annotation of genes (Mittal et al., 2019). Moreover, short fragments of assembled genomes are inconvenient in detecting genome-wide runs of homozygosity (ROH) and identity-by-descent (IBD), but this is critically relevant for assessing inbreeding for endangered animals.

Here, we assembled and annotated a South China tiger genome and upgraded an Amur tiger genome at the chromosome level by combining PacBio long reads sequencing, Hi-C technology, paired-end short reads sequencing and RNA sequencing (RNA-seq) data. We also resequenced 28 tigers of the two subspecies with at least 15-fold genome coverage per individual to support accurate analysis in this study. Notably, we characterized the architecture of the two genomes, and for the first time, demonstrate the decline in the effective population of the South China tiger, the Amur tiger, over the last 1000–10,000 years. Furthermore, we investigated the effects of inbreeding, patterns of heterozygosity loss, extremely homozygous fragments present on chromosomes, and genetic loads. As far as we know, this is the first report to evaluate the genome-wide inbreeding context of the South China tiger population, which will provide a new perspective for developing genetic management policies.

2 | MATERIALS AND METHODS

2.1 | Samples

Thirty tiger samples, including blood and tissue, were collected from zoos, including 14 Amur tigers (*Panthera tigris altaica*, AT) and 16 South China tigers (*P. t. amoyensis*, SCT). Blood samples from a male AT individual (from the China Hengdaohezi Feline Breeding Center) and a male SCT (from the Meihuashan South China Tiger Breeding Institute, China) were chosen for genome assembly. Samples from the remaining 28 individuals included skins, tissues and blood. Blood samples were obtained during physical examination. Skin and tissue samples were collected from individuals that died of natural causes and were preserved in zoo veterinary hospitals. The 28 samples were used for whole-genome resequencing.

2.2 | DNA extraction, library construction and sequencing

For PacBio sequencing, high-molecular-weight genomic DNA was extracted from blood samples using the DNeasy Blood and Tissue kit (Qiagen). According to the manufacturer' s instructions, an average insert size of 20-kb SMRTbell libraries were constructed using the SMRTbell Template Prep Kit 1.0 (Pacific Biosciences) and Blue Pippin (Labgene Scientific) was then used for fragment size selection. Library sequencing was performed by use of single molecule real-time (SMRT) sequencing (PacBio RSII) technology in the Genome Center of Novo Genomics (Tianjin, China).

For Hi-C sequencing, red blood cells were extracted from a 2-ml blood sample, and fixed with 37% formaldehyde. After incubating for 10 min at room temperature, 2.5 M glycine was added to terminate the cross-linking reaction, and the precipitated cells were collected. Two Hi-C libraries (Lieberman-Aiden et al., 2009) were prepared for each subspecies, and sequenced on the MGISEQ-2000 sequencer (MGI).

DNA samples used for short read resequencing (paired-end 100 bp) were extracted by using the standard phenol–chloroform method and quantification was performed by using a Nanodrop Spectrophotometer (Thermo). DNA libraries were constructed as per the manufacturer's instructions (MGIEasy universal DNA Library Preparation Kit, BGI). Libraries were sequenced on a DNBSEQ-T1 sequencer.

RNA was isolated from blood samples of SCT individuals using TRIzol reagent (Invitrogen), and the integrity was verified on an Agilent 2100 Bioanalyzer. The cDNA libraries were constructed according to the manufacturer's instructions (MGIEasy RNA Library Prep Kit, BGI), and finally sequenced on the DIPSEQ-T1 sequencer.

2.3 | Genome assembly

Genome sizes/characteristics of AT and SCT were estimated based on K-mer (17-mer) frequency. The chromosome-scale genome was assembled with PacBio long reads, DNBSEQ short reads and Hi-C sequencing data. The CANU (version 1.7) (Koren et al., 2017) pipeline was used for assembly of initial contigs as follows: (i) PacBio long reads with the length shorter than 1000 bp were filtered out; (ii) remaining long reads (AT: 112.28 times coverage, SCT: 55.55 times coverage) were subjected to CANU for read correction, read trimming and unit construction, with parameters of "*maximum thread = 104, corOutCoverage = 40*". Short reads derived from paired-end sequencing (~51×) were used for base correction using NEXTPOLISH (version 1.3.1) software (Hu, Fan, et al., 2020, Hu, Hao, et al., 2020) on the draft genomes. Subsequently, Hi-C reads from the two individuals were mapped to each of the two genomes by the Burrows–Wheeler Aligner (BWA, version 0.7.17) (Li & Durbin, 2010) software with parameters bwa *mem -t 16 -k 19* (*–t: number of threads; –k: minimum seed length*). The BWA mapping results were filtered via the Hi-C-Pro pipeline (Servant et al., 2015). Then, JUICER (version 1.5.7) (Durand et al., 2016) software was used to manually assist in correcting and reviewing the preliminary chromosomal mount results. Finally, the chromosome-level genome was generated by the 3D-DNA pipeline (Dudchenko et al., 2017) and named AmyTig1.0 and PanTig2.0, respectively. We then performed synteny analysis between the tiger genomes and the domestic cat (Felis_catus_9.0, GenBank assembly accession: GCA_000181335.5) genome downloaded from the NCBI website by using MINIMAP2 (version 2.22) (Li, 2018) software with the

parameters *-cx asm10* (*asm10: intra-species asm-to-asm alignment*). The chromosome IDs of autosomes and sex chromosomes in the AmyTig1.0 and PanTig2.0 genomes were then determined according to the synteny relationship with the cat genome.

2.4 | Evaluation of the quality of assembled genomes

Statistics of the genome assembly were analysed using QUAST (version 4.0) (Gurevich et al., 2013) (a python script), which gives detailed information for contigs and scaffolds of each tiger genome. BUSCO (Seppey et al., 2019) (version 3, mammalia_odb9, 4104 genes) analysis was performed to evaluate the completeness of the genome assembly. To further verify the quality and completeness of our genome assemblies, BWA (version 0.7.17) (Li & Durbin, 2010) (bwa *mem -t 8 -k 30 -M*) was performed and mapped the paired-end short reads to the two genomes, respectively. Genome mapping rate and sequencing coverage were obtained by SAMTOOLS (v1.4) (Li et al., 2009) with the parameter *-flagstat* and BAMDEAL (https://github.com/BGI-shenzhen/BamDeal) with statistical coverage command, respectively.

To further show the improvement in completeness and contiguity of our assembled genome, we investigated how many gaps in the PanTig1.0 genome could be filled by our assembled AT genome. We split the PanTig1.0 (Cho et al., 2013) genome into contigs by gaps and then mapped these contigs to our Amur tiger genome (PanTig2.0) through BLAT (version 35.1) software (Kent, 2002). The number and size of gaps in the PanTig1.0 genome filled by our assembled genome were calculated by a custom Perl script (https://github.com/cat1zhang/split-the-genome-to-contigs-by-gaps).

2.5 | Annotation of repeat elements

Repeat sequences in genomes of the two tigers were identified using a combination of homologue-based and *ab initio* prediction methods. REPEATMASKER (version 4.0.5) (Tarailo-Graovac & Chen, 2009) was used to search against the Repbase library (Jurka et al., 2005), followed by execution of REPEATPROTEINMASK (version 4.0.5) for homologue prediction. *Ab initio* prediction was performed using REPEATMODELER (version 1.0.4) (Smit et al., 2015). Additionally, TANDEM REPEAT FINDER (version 4.0.7) (Benson, 1999) was used to predict tandem repeats.

2.6 | Gene prediction and gene function annotation

Gene prediction was carried out on the homology-based, RNA-seq data and *de novo* gene prediction using repeat masked genomes. Homology-based prediction was performed by alignment of homologous proteins of five species including domestic dog (*Canis lupus familiaris*, GCF_000002285.3_CanFam3.1), human (*Homo sapiens*, GRCh38), Canadian lynx (*Lynx canadensis*, GCA_900661375.1_LYPA1.0), mouse (*Mus musculus*, GRCm38) and leopard (*Panthera pardus*, PanPar1.0) downloaded from "NCBI" and "Ensemble" 97 release to the two assemblies using the "TBLASTN" tool (BLASTALL version 2.2.26) (Mount, 2007) with an E-value set to 1×10^{-5}. The alignment hits were linked to candidate gene loci by SOLAR (version 0.9.6) (https://sourceforge.net/p/treesoft/code/HEAD/tree/branches/lh3/) and low-quality records (amino acid <30 bp) were filtered out. Second, GENEWISE (version 2.4.1) (Birney et al., 2004) was used to analyse the aligned sequences to predict gene models. In the *de novo* predictions, AUGUSTUS (version 3.2.1) (Keller et al., 2011), SNAP (version 1.0) (Korf, 2004), GLIMMERHMM (version 3.02) (Majoros et al., 2004), GENESCAN (Burge & Karlin, 1997) and GENEID (Parra et al., 2000) software were used to identify protein-coding genes in the two tiger genomes. Additionally, the raw RNA-seq of the SCT was filtered by TRIMMOMATIC (version 0.30) (Bolger et al., 2014) prior to transcript assembly. Since RNA-seq was not performed for the AT individual, RNA data used for transcripts assembly were downloaded from NCBI (SRR924676). Transcripts were aligned against assemblies using PASA (version 2.0.2) (Haas et al., 2008) and effective alignments were assembled to gene structures. Finally, all the above three data sets were combined to generate a nonredundant and comprehensive gene set using MAKER (version 1.0) (Cantarel et al., 2008).

Protein-coding gene motifs and domains were annotated by searching against InterPro (Apweiler et al., 2001) and KEGG (Kanehisa & Goto, 2000) public databases.

2.7 | Genome collinearity analysis and structural variant detection

Genomic structural differences between the newly assembled AT and SCT genomes were detected by collinearity analysis using the MCSCANX package (Wang et al., 2012). Single-nucleotide variants (SNVs) and small InDels on the two tiger genomes were called from short-read alignments by running the SENTIEON (Kendig et al., 2019) pipeline (Sentieon *driver -t 48 --algo GVCFtyper*). The Genome Analysis Toolkit (GATK, versio 4.0.3.0) (DePristo et al., 2011) software was used for splitting the SNVs (gatk *--java-options "-Xmx5g" SelectVariants --select-type-to-include SNP*) and InDels (gatk *--java-options "-Xmx5g" SelectVariants --select-type-to-include INDEL*). Structural variants were detected by SNIFFLES (version 1.0.6) (Sedlazeck et al., 2018). Briefly, ~30× SCT PacBio reads were mapped to the AT genome (PanTig2.0) and ~32× AT PacBio reads were mapped to the SCT genome (AmyTig1.0) using NGMLR (version 0.2.6) (Sedlazeck et al., 2018) with default parameters. After sorting the mapping files generated by NGMLR, SNIFFLES (version 0.2.6) was used for the detection of structural variants (SVs) larger than 50 bp with parameters "*-q 20 -l 50*."

2.8 | Variant calling and SNP filtering

TRIMMOMATIC (version 3.20) (Bolger et al., 2014) software was used to filter the low-quality reads and adaptors with parameters "*-phred33 ILLUMINACLIP: adapter. fa: 2:30:4:1: true LEADING:3*

TRAILING:3 SLIDINGWINDOW: 5:15 MINLEN:50." Clean reads were then mapped to the SCT genome (AmyTig1.0) by BWA-MEM (versio 0.7.17) (Li & Durbin, 2010) with default parameters. Sorting, reordering and read deduplication were performed via PICARD TOOLS (version 2.25.6) (https://github.com/broadinstitute/picard/releases/tag/2.25.6). SENTIEON (Kendig et al., 2019) with parameters *"driver -t 48 --algo GVCFtyper"* was finally used to generate the combined raw VCF files. To facilitate downstream analysis, we separated single nucleotide polymorphisms (SNPs) from InDels by GATK (version 4.0.3.0) (DePristo et al., 2011) software with the parameter "*SelectVariants --select-type-to-include SNP/INDEL*." The separated raw VCF files were filtered by: (i) hard filtration by setting "QD < 2.0 || FS > 60.0 || MQ < 40.0 || MQRankSum < −12.5 || ReadPosRankSum < −8.0"; (ii) removing all non-bi-allelic variants; (iii) variants with a Phred-scaled genotype quality score <20 were marked as low-quality; (iv) a variant with a proportion of low-quality and missing genotype larger than 10% were removed; and (v) removing variants with a minor allele frequency (MAF) less than 1%.

To identify and remove duplicate individuals, full siblings, or half-siblings from the 28 tiger samples, we performed the KING (version 2.2.5) (Manichaikul et al., 2010) software with the parameters "*KING -b xx.bed -fam xx.fam -bim xx.bim -m xx.map –related*" (bed, fam and bim files were generated by PLINK [version 1.09]; Purcell et al., 2007).

2.9 | Principal component analysis (PCA), admixture, phylogenetic tree and population differentiation (F_{ST}) analysis

PCA was carried out based on 6,289,055 SNPs to evaluate the genetic relationship between two tiger populations by using Genome-wide Complex Trait Analysis (GCTA, version 1.92.2) (Yang et al., 2011) software. PCA results were visualized using R (version 3.6.3) (Ihaka & Gentleman, 1996). A hierarchical Bayesian model in ADMIXTURE (version 1.23) (Alexander et al., 2009) was used to examine ancestral components of the 28 tiger individuals using the same SNP data set as in PCA with *K* values ranging from 1 to 5. The maximum-likelihood (ML) phylogenetic tree was constructed by using IQ-TREE (version 1.6.12) (Nguyen et al., 2015) with the following parameters: *-nt 4 -bb 1000 -alrt 1000 -m TEST -st DNA* (*−bb: bootstrap*). Weir and Cockerham's fixation index (F_{ST}) was calculated using VCFTOOLS (version 0.1.13) (Danecek et al., 2011) with parameters "*--fst-window-size 500,000 --fst-window-step 50,000*."

2.10 | Inference of demographic dynamics and divergence time

Estimation of the effective population size and inference of divergence time between the AT and SCT were carried out using MSMC2 (version 2.0.0) (Schiffels & Durbin, 2014) and SMC++ (v1.13.1) (Terhorst et al., 2017) software. For the inference of *Ne* by the MSMC2 method, we first phased the whole SNP set using BEAGLE (version 5.0) (Browning et al., 2018) with default parameters. Then we randomly selected four individuals from each population to infer the change of effective population with parameters "*-I '0,1,2,3,4,5,6,7' -i 20 -t 6 -p '1*2+15*1+1*2'*" (*-I, −−pairIndice*: give a list of phased haplotypes, and each number represents a haplotype. Here we represent four individuals with eight haplotypes; *−i, −−maxIterations*: number of EM-iterations; *−t, −−nrThreads*: number of threads we used; *−p, −−timeSegmentPattern*: pattern of fixed time segments). We randomly selected four individuals from each population for the inference of separation time of the two subspecies with following parameters: "*--skipAmbiguous -I 0–8,0-9,0-10,0-11,0-12, 0-13,0-14,0-15,1-8,1-9,1-10, 1-11, 1-12,1-13,1-14,1-15, 2-8,2-9,2-10,2-11,2-12,2-13, 2-14,2-15,3-8,3-9,3-10, 3-11,3-12,3-13,3-14,3-15,4-8, 4-9,4-10,4-11,4-12,4-13, 4-14,4-15,5-8,5-9,5-10,5-11,5-12,5-13,5-14,5-15,6-8,6-9,6-10,6 -11,6-12,6-13,6-14,6-15,7-8,7-9,7-10,7-11,7-12,7-13,7-14,7–15"* (*−−skipAmbiguous*: skip sites with ambiguous phasing; *-I: pairIndices*: give a list of haplotype pairs. In this case, the program will run with only those specified pairs of haplotypes). We performed five independent calculations for the inference of both *Ne* and separation time to guarantee the reliability. The generation time and mutation rate we used for scaling the results to the real time (year) were $g = 5$ years and $\mu = 0.3 \times 10^{-8}$ per year (Liu et al., 2018), respectively.

To further validate the results from MSMC2, we also performed SMC++ analysis to infer the dynamics of the effective population size with parameters "*--cores 8 --knots 26 --timepoints 40, 90,000*" (*−−knots*: the number of spline knots used in the underlying representation of the size history; *−−timepoints*: this command specifies the starting and ending time points of the model [in generations]), and the separation time between the two subspecies by using all 28 individuals.

2.11 | Genome-wide genetic diversity estimation

VCFTOOLS (version 0.1.13) (Danecek et al., 2011) was used to calculate the density of SNPs (*−−SNPdensity 50,000*) and estimate nucleotide diversity (π) (*−−window-pi 500,000 --window-pi-step 100,000*).

2.12 | Runs of homozygosity (ROH) analysis

PLINK (version 1.09) (Purcell et al., 2007) was used to prune the SNP set with parameters "*--indep-pairwise 50kb 1 0.9"* (*50kb*: the window size; *1*: step size [variant ct]; *0.9*: a pairwise r^2 threshold). The pruning process removed 3,974,190 of 6,289,055 variants. The remaining 2,314,865 SNPs were then used to analyse ROH by PLINK (Purcell et al., 2007) with parameters from Dobrynin et al. (2015) "*--homozyg-window-snp 20 --homozyg-kb 10 --homozyg-density 50*." The length of ROH and the expected generations were calculated with an average recombination rate of 1.1 cM per Mb which was roughly deduced from the domestic cat (Dumont & Payseur, 2008). The formula (Thompson, 2013) is:

TABLE 1 Statistics of our assembled genomes compared with the PanTig1.0 (Cho et al., 2013) and Maltig1.0 (Armstrong et al., 2021) genomes

Parameter	AmyTig1.0	PanTig2.0	PanTig1.0 (Cho et al., 2013)	Maltig1.0[a]
Largest scaffold (Mb)	238.2	237.5	41.6	–
Largest contig (Mb)	56.02	60.36	0.29	–
Contig N50 (Mb)	9.47 Mb	9.52 Mb	0.039	1.8
Scaffold Ns (%)	0.046	0.024	2.44	1.31
Scaffold N50 (Mb)	145.6	144.6	8.9	21.3
GC (%)	41.67	41.72	41.39	40.70
Total length (Gb)	2.5	2.5	2.4	2.4

[a]The data (Maltig1.0) come from the original article (Armstrong et al., 2021).

$$g = 100 / (2rL_{ROH})$$

where g = generation interval, r = recombination rate and L = length of the ROH (Mb).

F_{ROH}, the proportion of the autosomal genome in ROH (McQuillan et al., 2008), was calculated as:

$$F_{ROH} = \Sigma L_{ROH} / L_{AUTO}$$

where L_{ROH} = sum of ROH lengths, and L_{AUTO} = length of the genome covered by the genome-wide SNPs (L_{AUTO} = 2,258,664,721 bp).

2.13 | Detection of IBD segments

The proportion of pairwise shared IBD for all individuals, including intra- and intersubspecific pairs, was calculated using PLINK (version 1.09) (Purcell et al., 2007). Refined IBD (*refined-ibd.16May19.ad5.jar length = 1 window = 5*) (Browning & Browning, 2013) was used to identify genomic segments containing shared IBD segments among individuals with default parameters. The input file was created using VCFTOOLS (version 0.1.13) (Danecek et al., 2011) with parameters "*vcftools --gzvcf --max-missing 1 --maf 0 --recode --recode-INFO-all --stdout | tr '/' '|' |.*" Here we obtained variants with no missing genotypes for IBD calculation.

2.14 | Genetic load estimation

The evaluation of genetic loads focused mainly on deleterious nonsynonymous SNPs (nsSNPs) and the loss of functional (LOF) mutations in this study. All variants were annotated with ANNOVAR (Kai et al., 2010) and nonsynonymous missense mutations were rated via the Grantham Score (Grantham, 1974) ranging from 5 to 215. Mutations with Grantham Scores ≥150 were regarded as deleterious. LOF mutations in coding regions were identified using SNPEFF (v4.3)(Cingolani et al., 2012) by the following procedures: (i) a database was built with the genome and annotation files of the SCT with parameters "*java -Xmx40g -jar snpEff.jar build -gff3 -v south_tiger*"; (ii) we used SNPEFF to annotate SNPs of each individual with parameters "*Java -Xmx4g -jar snpEff.jar eff -c snpEff.config -v south_tiger*"; and (iii) we merged the stop gained, splice acceptor variant, splice donor variant as the final LOF mutations for downstream analysis.

To better present the genetic load, we calculated the ratio of homozygous sites (two per site) to both heterozygous (one per site) and homozygous sites (two per site) for both deleterious nsSNPs and LOFs for each individual following the method of Feng et al. (2019), with the formula: ratio = 2 * homozygous sites/(2 * homozygous sites +1* heterozygous sites). The homozygous sites represent the number of homozygous alleles (0/0 or 1/1) per individual, while heterozygous sites represent the number of heterozygous alleles (0/1) per individual.

3 | RESULTS

3.1 | *De novo* assembly and annotation of tiger genomes

One male adult SCT and AT were used for genome assembly (Table S1). The final SCT and AT assemblies were 2.45 and 2.46 Gb, representing 98.5% and 98.2% of their estimated size, respectively (Figure S2). The PacBio subreads were used to assemble the genome from scratch and the short paired-end reads were then used for base correction of our assembled draft genome. Subsequently, Hi-C data were used to locate the assembly sequence and orient the scaffold to the genome at the chromosome level. Finally, the scaffold N50 of two genomes was145.6 Mb (SCT) and 144.6 Mb (AT), suggesting that the two assemblies were dominant in terms of long fragments (Table 1; Tables S2 and S3, Figure S3).

In the Benchmarking Universal Single-Copy Orthologs (BUSCO) (Seppey et al., 2019) analysis, our assembled genomes covered 95.7% (SCT) and 95.5% (AT) complete BUSCO genes (Table S4), showing the completeness of the two tiger genomes. To further evaluate the quality of the genomes, the short reads generated for genome size estimation were mapped to their respective genomes, with 99.68% (SCT) and 99.77% (AT) of the sequencing reads mapped on the two genomes. Compared to the previously published PanTig1.0 (Cho

et al., 2013), our newly assembled AT genome filled 109,603 gaps, totalling 47.7 Mb, which accounted for 81.9% of the gaps in the PanTig1.0 genome (2% of the entire genome, Table S5). These indices clearly demonstrated the superior contiguity of our assembled genomes.

The total length and proportion of the repetitive elements were roughly equal between the two genomes, 910.94 Mb in SCT and 914.45 Mb in AT, accounting for 37.03% and 37.07% of the total genome, respectively (Tables S6 and S7). With the combination of transcriptome mapping, *ab initio* predictions and homology-based protein alignment approaches, a total of 18,751 and 18,497 protein-coding genes were predicted from the two genomes (Table S8, Figure S4).

The completeness of protein-coding gene sets was evaluated by BUSCO analysis, and the complete BUSCO scores were 95.8% and 95.7% for SCT and AT, respectively (Table S9). The number of genes was 18,751 in the SCT genome and 18,497 in the AT genome, 7.22% and 5.95% higher, respectively than that of PanTig1.0, which contains 17,391 annotated protein-coding genes. In the SCT genome, 95.37% of the protein-coding genes were found to be functional, while this was 95.57% in the AT genome (Figure S5, Table S10).

Global collinearity analysis showed ~97.8% of the SCT genome matched in one-to-one syntenic blocks to 97.9% of the AT genome (Table S11, Figure 1-1), demonstrating extremely high similarity between them. By mapping the genome survey data to the AT and SCT genomes, we found that the number of SNVs and small InDels in the SCT genome (1,490,015 and 371,740) were much lower than that in the AT genome (2,005,333 and 615,597) (Figure 1-5,6). Putative SVs > 50 bp detected in the SCT genome included 7286 deletions, 253 duplications, 7795 insertions and 73 inversions, while SVs detected in the AT genome included 2050 deletions, 65 duplications, 2209 insertions and 20 inversions (Figure 1-7,8; Figure S6).

3.2 | Subspecies separation and inference of recent demographic history

Fifteen SCT and 13 AT individuals were resequenced at an average depth of 20.34-fold (15.75–25.32-fold) (Table S12). All tigers were identified as unrelated individuals by kinship analysis, and their sequencing reads could be used for the analysis of downstream population genomics (Figure S7). By mapping resequencing data of the 28 tigers to our assembled SCT genome (AmyTig1.0), a total of 6,289,055 qualified SNPs and 964,481 INDELs were obtained (see Methods). To compare with previously published analysis (Liu et al., 2018), we also performed PCA, phylogenetic tree and admixture analysis. As expected, this supported that SCT and AT were two distinct groups (Figure S8) with a Weir and Cockerham's fixation index (F_{ST}) between SCT and AT populations of 0.29, falling in the intersubspecific range of tigers (0.20–0.32) (Armstrong et al., 2021).

Although the demographic history of tigers has been extensively explored (Armstrong et al., 2021; Cho et al., 2013; Liu et al., 2018), details of the population history within the last 10,000 years are largely unknown, especially for the SCT, due to the limitation of sampling and analysis methods. MSMC (Stephan Schiffels & Wang, 2020) and SMC++ (Terhorst et al., 2017) have been shown to be effective at inferring more recent population histories (Guang et al., 2021; Schiffels & Durbin, 2014). Therefore, the recent historical dynamics of effective population size (*Ne*) and separation time between the two subspecies were inferred using MSMC2 (Stephan Schiffels & Wang, 2020) and SMC++ (Terhorst et al., 2017) in this study. The results indicated that the *Ne* of SCT and AT experienced a similar evolutionary trend, a dramatic decline followed by a slow and gradual reduction until the end of the Holocene optimum (~5000 years ago) when the reduction rate in the SCT became sharper than in the AT and reached a minimum by ~800 years ago (Figure 2a,b; Table S13). The separation between SCT and AT subspecies was inferred around 7000 years ago according to the results from MSMC and SMC++ (Figure 2c,d). This supports the hypothesis that the AT population originated less than 10,000 years ago, based on microsatellite and mitochondrial data (Driscoll et al., 2009; Luo et al., 2004). However, the separation at 7000 years ago should be further validated with ancient tiger samples in the future.

3.3 | Genetic diversity maintained in the current population

The SNP density (number of variants per kb) of the SCT population averaged 1.60 ± 1.04, lower than that in the AT population (2.60 ± 1.34) (Figure 3a). Nucleotide diversity (π) of the SCT population (from 1.33E−07 to 0.002, mean = 0.00058 ± 0.00029) was also lower than that in the AT population (from 2.63E−06 to 0.0023, mean = 0.0008 ± 0.0003) (Figure 3b). This result is consistent with PCA in which SCT is more concentrated than AT (Figure S8a).

3.4 | Genomic signature of inbreeding

3.4.1 | ROH fragments on genomes

ROH was analysed for 18 autosomes. A total of 5407 ROHs were identified in the SCT population, and 4262 in the AT population. The length of ROH ranged from 47.9 kb to 58.9 Mb in the SCT population, and from 42.9 kb to 36.3 Mb in the AT population (Figure S9). ROH on SCT genomes were long and continuous, covering a greater portion of chromosomes compared to AT (Figure 4a). The proportion of ROH counts ≥1 Mb (resulting from recent inbreeding events; Yoshida et al., 2020) in total ROH ranged from 0.361 to 0.599 per individual and averaged 0.433 in the SCT population. This was significantly greater than that in the AT population, which ranged from 0.183 to 0.433 per individual and averaged 0.31 at the population level (Studentps *t* test, $p = 9.14E{-}05$, Figure 4b; Table S14).

Mean inbreeding coefficient ($F_{ROH,}$ proportion of ROH in the genome) (Alemu et al., 2021) was also much higher in SCT ($F_{ROH} = 0.40 \pm 0.077$) than in AT ($F_{ROH} = 0.21 \pm 0.041$, Student's *t*

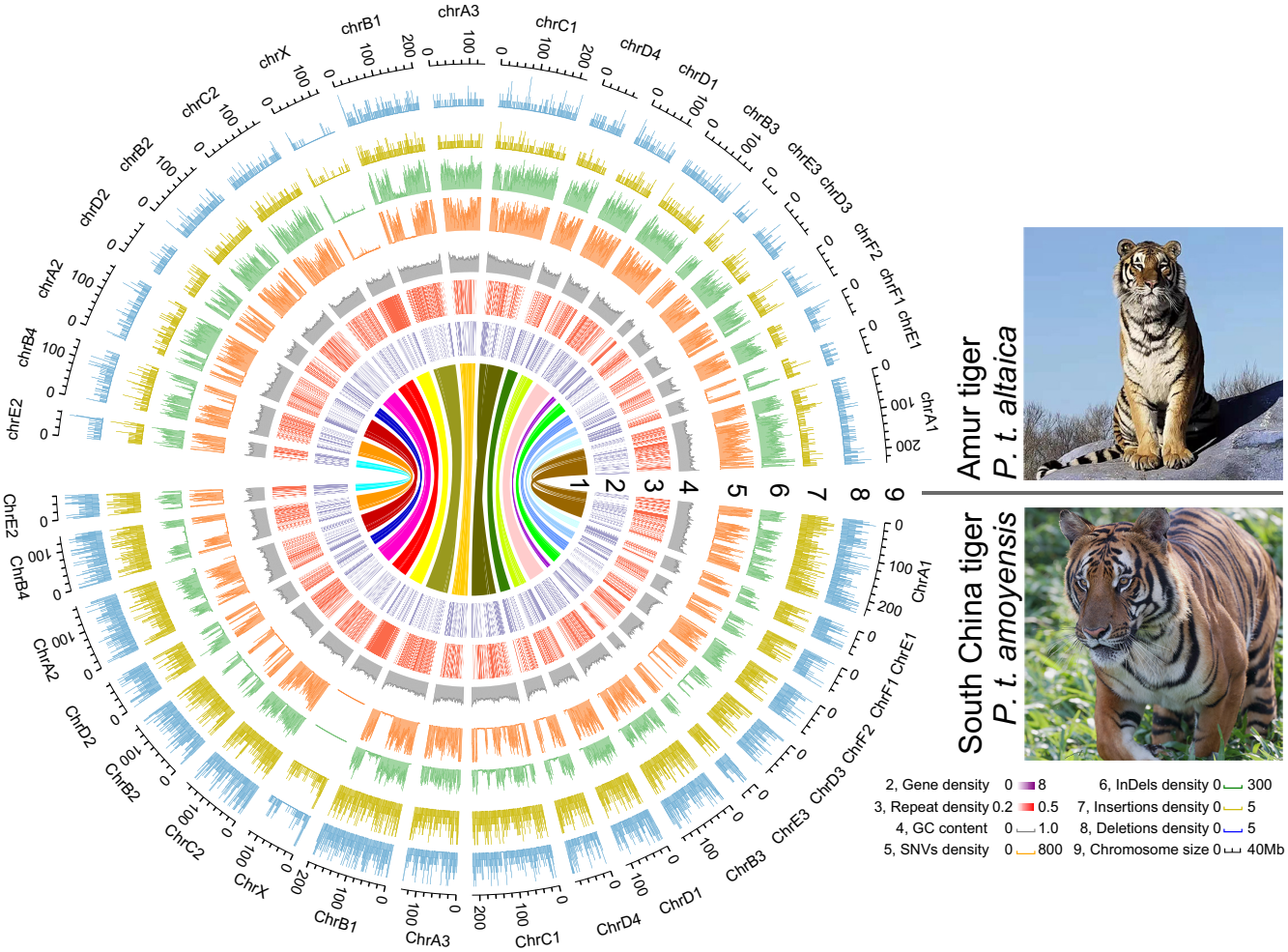

FIGURE 1 Overview of the two tiger genomes. Components and structural distribution of Amur (upper) and South China (lower) tiger genomes. 1. Collinearity of the two tiger genomes. 2. Distribution of genes. 3. Distribution of transposons in repeat elements. 4. Density of GC content. 5. SNV distribution in the two genomes. 6. Density of short InDels between the two genomes. 7. Density of large insertions (>50 bp). 8. Density of large deletions (> 50 bp). 9. Chromosomes of the two subspecies

test, p = 1.41E−08) (Table S15). Genomic heterozygosity was negatively correlated with F_{ROH} in both SCT (R = −0.99, p = 4.8e−12) and AT (R = −0.97, p = 2.9e−08) (Figure 4c). Correspondently, genomic heterozygosity was positively correlated with the length of non-ROH regions in the genome of both SCT (R = 0.99, p = 4.8e−12) and AT (R = 0.97, p = 2.9e−08) (Figure S10).

The history of inbreeding was inferred by calculating the number of generations (g) in which ROH occurred. The proportion of ROH <5 Mb was more predominant in AT (0.93 ± 0.33) than SCT (0.85 ± 0.05) (p = 7.01E−05). The proportion of ROH >5 Mb in SCT was as high as 15%, while this proportion was only 7% in AT (Figure 4d,e; Table S14). It can be estimated that ROH >5 Mb originated within the recent 9.1 generations (see Methods). The generation length in the captive SCT is 7.3 years (estimated based on studbook). Therefore, such a large ROH should come from the past 66 years. The first breeding of SCT in captivity took place in 1972. It could be expected that inbreeding had started at the beginning of captive breeding and contributed to the loss of genetic diversity over time.

When the union of individual ROH was obtained by pooling conspecific genomes and removing redundant fragments, the proportion of total ROH length to the autosomes reached 94.7% in the SCT and 88.2% in the AT population (Figure S11). We further observed that the tested SCT population contained 323 ROH with an average length of 6.6 Mb, while the AT population contained 715 ROH with an average length of 2.8 Mb.

Moreover, we did not find any ROH shared by all individuals in the AT population, while the SCT population had an intersection containing 43 of all ROH that were 10.8 Mb in average size and 466 Mb in total length (Figure S12). We even observed eight

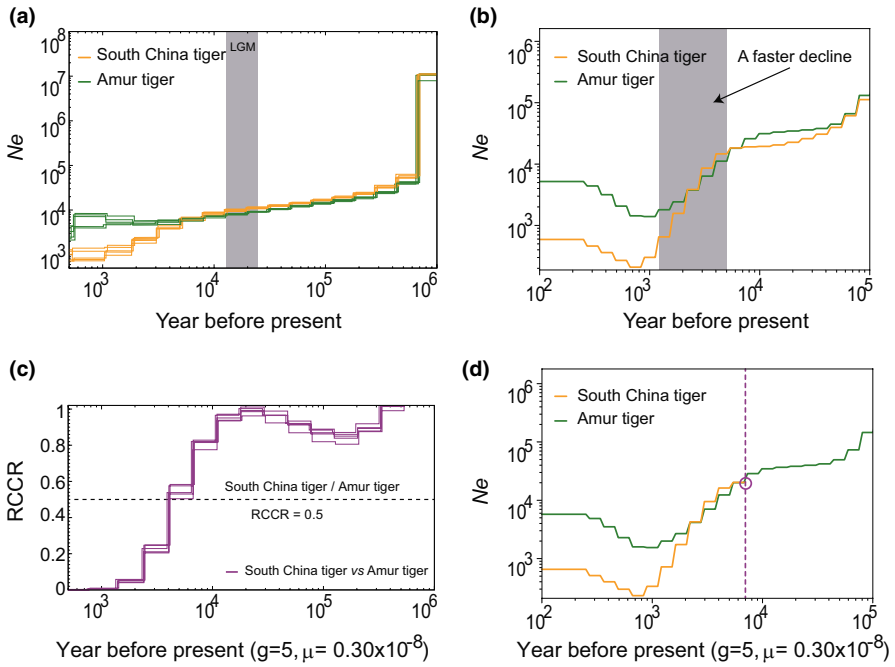

FIGURE 2 Demographic history and separation of the two tiger subspecies. (a) The effective population size of the two subspecies estimated using MSMC2 software by five independent calculations (four individuals were used in each calculation). (b) Effective populations estimated by SMC++ software using all 28 individuals. (c) Divergence time between the two subspecies estimated using MSMC2 software by relative cross-coalescence rate. The grey broken line indicates the separation of these two subspecies. (d) Time of split of the two subspecies inferred by SMC++ software. The purple broken line and circle is the inferred time point of separation of SCT and AT

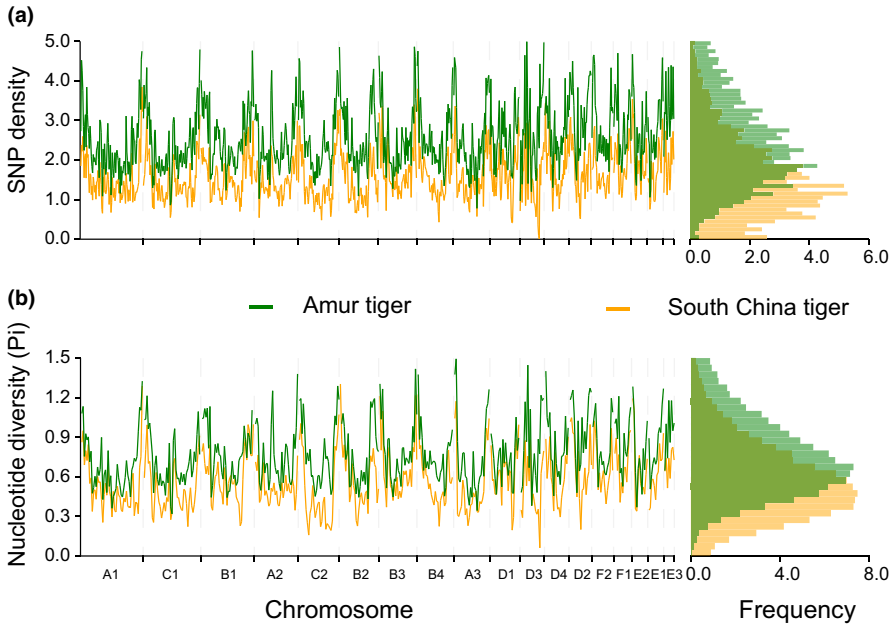

FIGURE 3 Genetic diversity in contemporary populations of the Amur and South China tiger. (a) Statistics of SNP density (50-kb nonoverlapping window calculation) in the two tiger populations. (b) Distribution of nucleotide diversity ($\pi \times 1000$) in the two tiger populations

shared ROH segments spanning 91.5 Mb on ChrB4 in the SCT population, and this represented 65.63% of the total ChrB4 length. GO categories showed that the genes covered by the ROH intersection in the SCT population were involved in sensory perception of taste (GO:0050909, $p = .00308$), interleukin-1 receptor binding (GO:0005149, $P = 0.0106$), growth factor receptor binding (GO:0070851, $p = .0286$) and ephrin receptor activity (GO:0005003, $p = .0196$) (Table S16), etc., suggesting ROH may potentially influence

FIGURE 4 Heterozygosity and ROH in Amur tigers and South China tigers. (a) Distribution of individual heterozygosity and ROH on chromosomes. Black irregular lines indicate the distribution of individual heterozygotes, and green and yellow short vertical bars represent ROH larger than 1 Mb in the SCT and AT populations. (b) Count of ROH of different lengths in the AT and SCT populations. (c) Average genome-wide heterozygosity vs. F_{ROH} in AT (green) and SCT (yellow). (d) The ratio of ROHs >5 Mb and ROHs <5 Mb to the total ROH counts per population (Statistical test method, two-tailed *t* test. The ratio of ROH count <5 Mb = 1 − ratio >5 Mb). (e) The ratio of total ROHs >5 Mb and ROHs <5 Mb to the total length of ROH per population in AT (green) and SCT (yellow) (Statistical test method, two-tailed *t* test, Error bars are ±SD. The ratio of ROH length <5 Mb = 1 − ratio >5 Mb

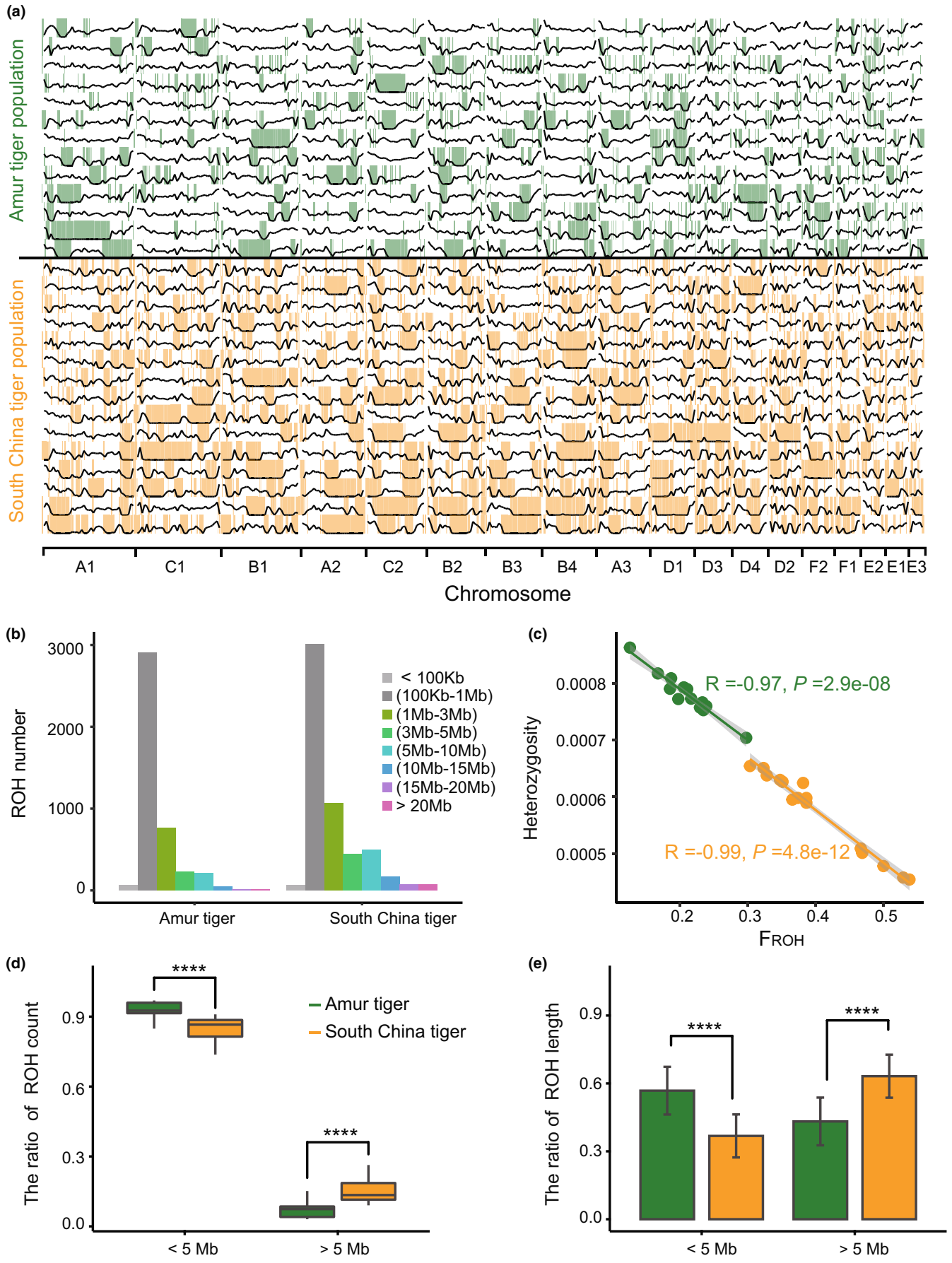
(a)
Amur tiger population
South China tiger population
A1
C1
B1
A2
C2
B2
B3
B4
A3
D1
D3
D4
D2
F2
F1
E2
E1
E3
Chromosome
(b)
ROH number
3000
2000
1000
0
< 100Kb
(100Kb-1Mb)
(1Mb-3Mb)
(3Mb-5Mb)
(5Mb-10Mb)
(10Mb-15Mb)
(15Mb-20Mb)
> 20Mb
Amur tiger
South China tiger
(c)
Heterozygosity
0.0008
0.0007
0.0006
0.0005
R =-0.97, P =2.9e-08
R =-0.99, P =4.8e-12
0.2
0.3
0.4
0.5
FROH
(d)
The ratio of ROH count
0.9
0.6
0.3
0.0
****
****
Amur tiger
South China tiger
< 5 Mb
> 5 Mb
(e)
The ratio of ROH length
0.9
0.6
0.3
0.0
****
****
< 5 Mb
> 5 Mb

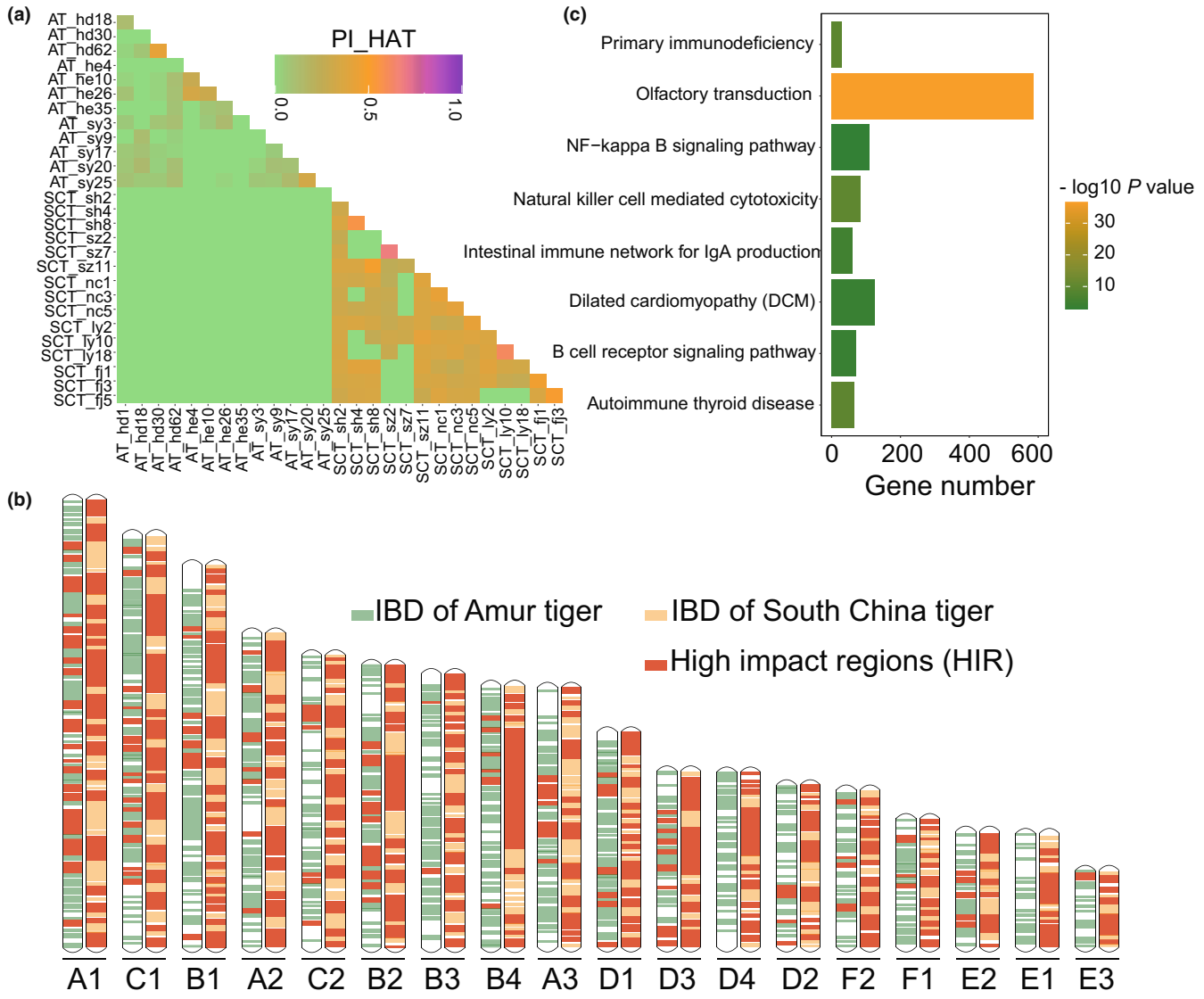

FIGURE 5 IBD segments shared in the SCT and AT subspecies. (a) Heat map of shared IBD by pairs of individuals, with PI_HAT representing the proportion of IBD. (b) Distribution of IBD regions in SCT and AT populations on 18 autosomes. For each chromosome, AT is arranged on the left (IBD shown as green) and SCT on the right (IBD shown as yellow). The orange blocks represent HIRs. (c) The KEGG pathway enrichment of genes covered by HIR of the SCT population

the performance of sensory perception, immunity, histogenesis and cell viability of the SCT.

3.4.2 | Homologous IBD segments

A total of 36,569 IBD fragments >1 Mb were identified in the SCT population and 4627 in the AT population. As shown in Figure 5(a), the proportion of IBD shared by arbitrary pairs of individuals was 0.28 ± 0.16 for SCT, 0.06 ± 0.08 for AT and 0 for SCT–AT pairs (Table S17). We regarded IBD regions shared by more than half of the individuals in each subspecies as high-impact regions (HIRs) (Feng et al., 2019). A total of 490 HIRs covering 1.98 Gb were identified in SCT, while only 179 HIRs were identified in AT, coving 505.6 Mb (Figure 5b). As shown in Figure 5(b), the number and continuity of HIRs on each putative chromosome were significantly greater in SCT than in AT. In particular, a large continuous HIR on ChrB4 of SCT (ChrB4: 52,559,777 to ChrB4: 116,658,974) even covered 580 genes. This indicated that IBD-associated influences are common in these chromosomal regions and irreducible for most pairing regimes in the present SCT population.

KEGG analysis showed that HIR-covered genes in the SCT (Figure 5c) are involved in natural killer cell-mediated cytotoxicity (map04650, $p = 9.81E{-}11$), primary immunodeficiency (map05340, $p = 1.95E{-}10$), B cell receptor signalling (map04662, $p = 9.60E{-}05$) and NF-kappa B signalling pathway (map04064, $p = 1.10E{-}03$). These results suggested that the homozygosity of these IBD regions may potentially influence the immunity-related performance of SCT.

3.4.3 | Putative genetic loads and distribution

To explore the potential influence of inbreeding on the quantity and distribution of genetic loads, we screened deleterious mutations using the population data, including deleterious nsSNPs and LOF mutations. The average number of nsSNPs on each genome was 6549 ± 671 for SCT and 10,489 ± 135 for AT (p = 1.06E−17, Student's t test) (Table S18). The number of deleterious nsSNPs (Grantham scores ≥150) identified on each genome was 465 ± 49 for SCT and 712 ± 15 for AT (p = 1.23E−15, Student's t test) (Table S18). However, the ratio of deleterious nsSNPs to total nsSNPs was 0.071 ± 0.002 for SCT and 0.068 ± 0.001 for AT (p = 1.91E−06, Student's t test) (Figure 6a; Table S18). On average, the deleterious nsSNPs were distributed on 657 ± 14 genes in the AT population and 438 ± 45 genes in the SCT population (Table S18). The ratio of deleterious nsSNP in a homozygous state was 0.47 ± 0.09 in SCT, significantly lower than that in the AT population (0.58 ± 0.029, p = 1.51E−04) (Figure 6b; Table S18). The deleterious nsSNPs were distributed on 1263 genes in the AT population and on 828 genes in the SCT population. For the SCT population, 719 genes lay in the ROH >5 Mb, while 630 genes fell in ROH ≥5 Mb for the AT population (Figure 6c,d). For the two subspecies, the density of deleterious nsSNP in ROH regions was significantly lower than in non-ROH regions (Figure S13), but the difference was greater in SCT (p = 2.54E−17) than in AT (p = 2.06E−04).

Similarly, three types (Feng et al., 2019) of LOF mutations were identified, including the stop gained mutation, splice acceptor variant and splice donor variant. A total of 713 LOF mutations were identified in SCT affecting 660 genes, and 519 LOF mutations identified in AT affecting 490 genes (Tables S19 and S20). All affected genes of AT were included in the affected genes of SCT. In particular, we examined the 170 SCT-specific affected genes and found several of them were related to reproduction, growth and development, disease, etc. For instance, the *STX2* (Fujiwara et al., 2013), *NANOS1* (Kusz-Zamelczyk et al., 2013), *ATAT1* (Yanai et al., 2020), *DNAH8* (Yang et al., 2020), *DNAH2* (Li et al., 2019) and *JMJD1C* (Kuroki et al., 2013) genes play important roles in sperm genesis, maturation and motility. *MyH10* (Kim et al., 2018), *CP* (Fleming & Gitlin, 1990), *RCOR1* (Yao et al., 2014), *DENND1A* (Shi et al., 2019), *RAD51D* (Pittman & Schimenti, 2000) and *PAPPA2* (Fujimoto et al., 2020) were related to fetal growth and survival. Deletions or mutations in *SKOR2* (Wang et al., 2011), *GNAO1* (Danti et al., 2017), *GFRA1* (Arora et al., 2021), *ARHGAP25* (Lindner et al., 2020), *SALL2* (Kelberman et al., 2014), *ABCB5* (Bruce et al., 2014) and *MYOF* (Doherty et al., 2005) would lead to abnormal growth of tissues and organs (Table S21).

The proportion of LOF mutations in the homozygous state was 0.51 ± 0.10 in the SCT population, slightly lower than that in the AT population (0.60 ± 0.03, p = 3.05E−03) (Figure 6b; Table S22). For both subspecies, the density of deleterious LOFs in ROH regions did not differ from that in non-ROH regions (Figure S13), but was greater in SCT than in AT. Overall mutational loads of nsSNP and LOF (AT/SCT) in ROH regions was 1.49 times higher than for non-ROH regions (Figure S14). The lower number of mutational loads in ROH regions and higher number in the non-ROH regions for the SCT compared to the AT could, to some extent, reflect the purging effects in the SCT.

4 | DISCUSSION

4.1 | High-quality genomes of the SCT and AT

Genetics has a long history of application in wildlife conservation (Frankham, 1995). Whole-genome sequencing techniques and analysis of population genetics have provided new insights into the consequences of revealing population history, population structure and genetic diversity (Barbosa et al., 2020). In particular, information on genome-wide variations is critical for researchers to advance their efforts to manage and conserve wildlife populations. In this study, we assembled the SCT genome named AmyTig1.0 and an AT genome named PanTig2.0 using the CANU assembler and a combination of long-read sequencing (PacBio), Hi-C and short-read (paired-end) sequencing technology. Compared to the PanTig1.0 and Maltig1.0 genomes, our genomes have greater scaffold continuity and completeness (Table 1; Table S4), fewer gaps (Table S5) and more BUSCO genes annotated (Table S9). The two chromosome-level genomes provide a firm basis for current and future studies on tiger biology and conservation.

4.2 | Three phases of effective population decline in SCT

Understanding the dynamics of effective population size of a species is critical for conservation. Our genomic analysis demonstrated that the SCT experienced three phases of effective population declines. The first occurred from ~5.0 to 1.0 thousand years ago when *Ne* reduced gradually from ~14.7 thousand individuals to ~200 individuals (Figure 2a,b). The second decline was in tha last 100 years. In this phase, human activity impacted almost the entire SCT range, leading to massive habitat loss (Miao et al., 2013; Yang & He, 2017). Together with hunting, the census population size was estimated to have fallen from ~4000 to functional extinction by the end of 1990s (Tilson et al., 1996; Tilson et al., 2004). No specimen from this period has yet been tested for genetic diversity. Nevertheless, this is the initial level of genetic diversity of the captive population. ROH with long sizes are associated with recent parental relatedness (Rosenberg et al., 2013). In the SCT population, 15% ROH were >5 Mb (Figure 4d,e; Table S14), suggesting inbreeding in the last nine generations, around 66 years ago, had led to a great deal of the loss in effective population size. The first breeding of SCT in captivity took place in 1963. Therefore, it could be expected that inbreeding

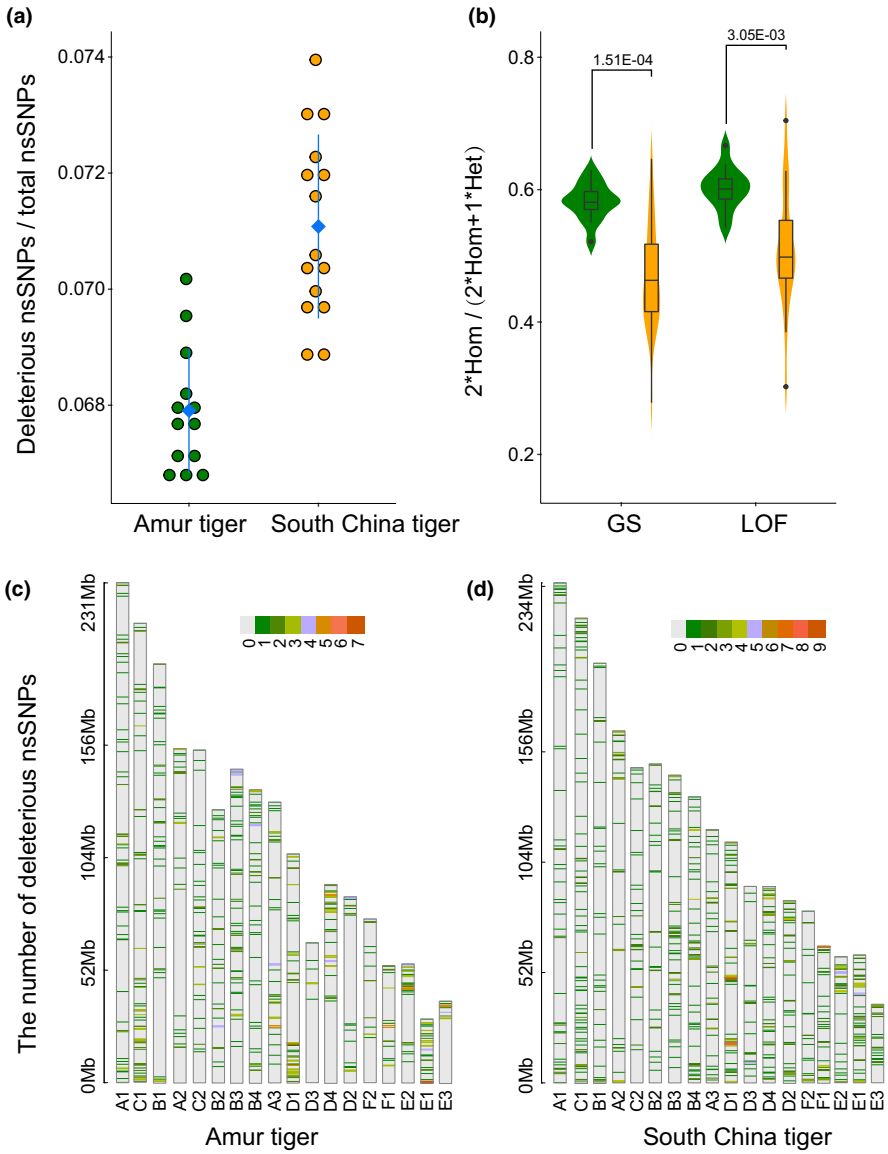

FIGURE 6 Genetic loads on the genomes of the SCT and AT subspecies. (a) The ratio of deleterious nsSNPs to total nsSNPs in the two tiger populations. Blue blocks and vertical lines are the mean and median values. (b) Summary of the two types of genetic load in the AT (green) and SCT (yellow) populations. GS represents the Grantham score, which was used for estimating deleterious nsSNP mutations, and LOF indicates the loss-of-function mutations. The box plot represents the overall distribution of the data, and the lines in the boxes represent the mean value. (c) Distribution of deleterious nsSNP site within ROHs >5 Mb in the AT population (window width 1 Mb). (d) Distribution of deleterious nsSNP sites within ROHs >5 Mb in the SCT population (window width 1 Mb)

had started at the beginning of captive breeding and, as the third phase, added to genetic diversity loss throughout history.

4.3 | Genome consequences of inbreeding depression in the SCT population

Two sorts of inbreeding depression have been recognized in the current SCT population, high juvenile, especially neonatal mortality (Yuan et al., 2021) and impaired adult fertility (Yuan et al., 2020; Yuan et al., 2021). In contrast, the extent of this inbreeding depression is slight in AT (Liu et al., 2013). We observed that ROH and IBD segments on SCT genomes were greater in number, mean size and total length than on AT genomes (Figures 4a,b and 5a,b). The longest IBD even spanned 580 genes on chromosome B4. Long ROH are probably the result of recent inbreeding, and the long IBD suggests that segments coming from common ancestors also accumulated progressively on the genome as a result of inbreeding (Hu, Fan, et al., 2020, Hu, Hao, et al., 2020; Kardos et al., 2018; Saremi et al., 2019).

We further screened two types of genetic load, deleterious nsSNPs and LOF mutations. Compared to AT, SCT had a relatively small number of deleterious nsSNPs and affected genes on genomes. However, the ratio of these nsSNPs to total nsSNPs was high compared to AT (p = 1.91E−06) (Figure 6a), implying that the SCT bears a high genetic load relative to total genetic variation, though the absolute quantity of deleterious nsSNPs is low. It should also be noted that the small number but low homozygosity of deleterious mutations in SCT (Figure 6b) suggest a mild purging mechanism in this population. In contrast to nsSNP loads, LOF loads seemed to be affected extensively in SCT. The number of genetic loads and the number of affected genes were 1.6 and 1.3 times greater than that in AT, respectively. We noticed that a few affected genes specific to the SCT were related to reproduction,

growth and development, and disease, etc. (Table S21), and some LOF mutations tend to impair sperm genesis, maturation and activity, fetal growth, and survival, as well as normality of tissue and organ development. This is consistent with the observed low reproductive rate and high cub mortality in the captive SCT population (Xu et al., 2007; Yuan et al., 2021).

Regarding to the interaction between inbreeding and genetic loads, comparison showed that, for deleterious nsSNPs, the total number in non-ROH regions was significantly greater than in ROH regions for both AT and SCT, and the number in ROH was even much lower than in non-ROH for SCT (Figure S13). This suggested that this type of genetic load is probably being purged by inbreeding in both subspecies, but the purging effect is stronger in SCT. However, SCT and AT did not show apparent purging effect as such for LOF (Figure S13).

4.4 | Insights from the genome into the genetic management of the SCT

Loss of genetic diversity and inbreeding of small populations are major threats to many wildlife populations (Hohenlohe et al., 2021). Research confirms that good management of captive populations of endangered species can help improve or sustain the gene pool, which is the last guarantee against the extinction of a subspecies in the wild (Christie, 2010). For conservation of such a problematic population, we propose some recommendations based on this study.

Our population genomic analyses indicate that the SCT population has many highly shared long ROH and IBD fragments caused by inbreeding (Figure S12; Figure 5b). Given that the level of inbreeding would incraese progressively without including outbred individuals in a breeding programme (Yuan et al., 2021), it is likely that the population would have a greater chance to have longer and more commonly shared ROHs and IBDs and suffer from consequent deleterious effects. Although there is limited operational space to slow down this process by the current pedigree-based distant relative pairing, it still deserves efforts. With reference to our high-quality genome, resequencing and comparison of individual genomes would facilitate accurate prediction of outcomes of pairing regimes. Practical methods need to be developed for this purpose.

The essential deleterious effects brought by inbreeding is exposure of genetic loads to a homozygous state. From a management point of view, it is apparent that recovering the SCT should primarily target genetic loads, either removing them or conceiving them in a heterozygous state. We observed that SCT may purge deleterious nsSNPs by inbreeding depression. However, the purging effect was not apparent for LOF. Meanwhile, unlike wild tigers (Khan et al., 2021), captive breeding might have relaxed purging strength through improvements of husbandry due to diet, feeding, environmental and behavioral enrichment, cub rearing and veterinary care (Li et al., 2013; Liu et al., 2014; Ma et al., 2020; Xu et al., 2021). Careful distant relative pairing (Yuan et al., 2021) also reduces, though only slightly, the chance of expression of deleterious variants as homozygotes. Therefore, purging may not be effective as expected to regain population quality. In addition, purging by inbreeding may lead to further loss of already low genetic diversity and increase the extinction risk (Caballero et al., 2017). For these reasons, management should not place great expectations on a purging approach.

Genetic rescue is an effective approach to break the negative cycle of inbreeding-depression by introducing genes from related species, subspecies and populations (Hedrick & Fredrickson, 2010). It has been taken into conservation practice for several species/populations (Fredrickson et al., 2007; Hasselgren et al., 2018; Weeks et al., 2017) and guidelines have been proposed based on the experiences obtained (Hedrick & Fredrickson, 2010). The applicability of genetic rescue to SCT has not yet been formally proposed. Nevertheless, our study provides some concerns before the strategy finally becomes an option.

From our genomic data, we inferred the divergence between AT from SCT started ~20,000 years ago and was completed ~7000 years ago (Figure 2c,d). Approximately 97.8% of the SCT genome matched in one-to-one syntenic blocks to 97.9% of the AT genome (Table S11; Figure 1-1), in which similarity even reached 99.2% in coding regions (Table S11). High genomic similarity in both sequence and organization suggests the potential of AT to be the gene donor. Furthermore, most ROH on SCT genomes are normal on AT genomes (Figure 4), and no IBDs were shared between the two subspecies (Figure 5a; Table S17). Deleterious nsSNPs and LOFs make up a small proportion of the total nsSNPs and LOFs in AT genomes and are distributed at low density compared with SCT genomes (Figure 6c). These imply that introduction of AT genes into the SCT gene pool would result in extensive heterozygosity throughout the genome to mask a great proportion of the genetic loads with normal alleles, from which offspring may benefit.

However, the presence of genes favouring cold adaptation on the genome of AT (Armstrong et al., 2021; Cho et al., 2013; Liu et al., 2018) may be functionally contradictory to the adaptation of SCT to warm climates. These genes might become novel genetic loads for the SCT gene pool given they are introduced. In view of these benefits and risks, the choice of donor subspecies for genetic rescue needs to consider aspects of genome similarity, ROH/IBD reduction, genome heterozygosity (especially for genetic loads) and most cautiously the introduction of novel genetic loads. In this regard, another close subspecies, the IndoChinese tiger, should also be included in the evaluation, because it inhabits subtropical areas south of the SCT and might have similar climate adaptations.

5 | CONCLUSIONS

This study assembled and characterized the first version of the SCT genome and an improved version of the AT genome. Inference from the genomes and small population resequencing data showed the effective population of SCT declined since its separation from AT

~7000 years ago Inbreeding of SCT started before captive breeding and has resulted in extensive distribution of long ROH, IBDs, deleterious nsSNPs and LOF mutations throughout the genome. Captive breeding has purging effects on genetic loads but cannot substantially restore the genetic quality. Current distant relative pairing and genome-based precise pairing would slow but not stop the progressive increase in inbreeding. Genetic rescue could be taken into consideration for SCT, but genome-based evaluation of donor subspecies should be made based on aspects of genome similarity, ROH/IBD reduction, genome heterozygosity especially for genetic loads, and most cautiously the introduction of novel genetic loads.

AUTHOR CONTRIBUTIONS

Y.C.X., T.M.L., L.Z., W.Y.F., Y.H.Y., H.L., X.X. and H.M.Y designed and managed the project. K.X.L., Z.Y.L., D.Q.C., X.H.W., S.Z.L., X.Z.W. and D.L provided and collected samples. L.Z. and X.T.R. extracted and isolated DNA. H.R.L., Y.T.H., J.Y.Y., Q.W. and S.F.Z. performed library construction and sequencing. Q.X.L. and A.S.W. analysed pedigree data and collected information of the SCT population. L.Z., D.M.F., T.M.L. and Y.C.X. performed the genomic analyses and created the Figures. H.M.L., X.T.R. and B.Y.L. assisted with processing and analysing the genomic data. Y.M. and Y.X.Z. prepared the data. L.Z., T.M.L. and Y.C.X. drafted and edited the manuscript. S.K.S. undertook manuscript proofreading and language editing. All authors contributed to discussions of the results and manuscript revision.

ACKNOWLEDGEMENTS

This work was supported by the Fundamental Research Funds for the Central Universities (2572020DR10) and the Guangdong Provincial Key Laboratory of Genome Read and Write (grant no. 2017B030301011), Siberian tiger Conservation Project of Forestry and Grassland Department of Heilongjiang Province, China. For indispensable assistance we thank Jianyi Yu and Guangyao Geng from Shanghai Zoo, Linxiang Li, Xing Liu and Yan Zhang from Suzhou Shangfangshan Forest Zoo, Hua Chen from Nanchang Zoo, Wu Chen from Guangzhou Zoo, Haitao Xu and Ming Gong from the Heilongjiang Siberian Tiger Park, Tengteng Chen and Zuomin Lan from Fujian Meihuashan Institute of South China Tiger Breeding, and Chang Su and Xin Mou from Northeast Forestry University with sample collection and securing transportation. We also thank Fengping He and Xiaofang Cheng for experimental assistance, Shangchen Yang and Lei Han for their valuable advice on bioinformatic analyses, and Kuo Xu for manuscript proofreading. We are especially grateful to Nonglin Liu, Zhong Xie and Zeying Yu from Chinese Association of Zoological Gardens and members of the Coordination Committee for South China Tiger Conservation for their unremitting efforts to support South China tiger studies. This work was supported by China National GeneBank (CNGB).

CONFLICT OF INTEREST

The authors declare that they have no conflicts of interests.

DATA AVAILABILITY STATEMENT

The genome assembly data of the two tigers are deposited in the China National GenBank (CNGB, https://db.cngb.org/cnsa/), the accession number is CNP0001654. The registration number of 28 tigers used for re-sequencing analysis is CNP0001906.

ORCID

Le Zhang https://orcid.org/0000-0002-4378-6053

REFERENCES

Alemu, S. W., Kadri, N. K., Harland, C., Faux, P., & Druet, T. (2021). An evaluation of inbreeding measures using a whole-genome sequenced cattle pedigree. *Heredity*, *126*(3), 410–423.

Alexander, D. H., Novembre, J., & Lange, K. (2009). Fast model-based estimation of ancestry in unrelated individuals. *Genome Research*, *19*(9), 1655–1664.

Apweiler, R., Attwood, T. K., Bairoch, A., Bateman, A., Birney, E., Biswas, M., & Croning, M. D. (2001). The InterPro database, an integrated documentation resource for protein families, domains and functional sites. *Nucleic Acids Research*, *29*(1), 37–40.

Armstrong, E. E., Khan, A., Taylor, R. W., Gouy, A., Greenbaum, G., Thiéry, A., & Barsh, G. (2021). Recent evolutionary history of tigers highlights contrasting roles of genetic drift and selection. *Molecular Biology and Evolution*, *38*(6), 2366–2379.

Arora, V., Puri, R. D., Ferreira, C. R., Verma, I. C., & El-Hattab, A. W. (2021). Biallelic pathogenic GFRA1 variants cause autosomal recessive bilateral renal agenesis. *Journal of the American Society of Nephrology*, *32*(1), 223–228.

Barbosa, S., Hendricks, S. A., Funk, W. C., Rajora, O. P., & Hohenlohe, P. A. (2020). Wildlife population genomics: Applications and approaches. In P. A. Hohenlohe & O. P. Rajora (Eds.), *Population genomics: Wildlife* (pp. 3–59). Springer.

Benson, G. (1999). Tandem repeats finder: A program to analyze DNA sequences. *Nucleic Acids Research*, *27*(2), 573–580.

Birney, E., Clamp, M., & Durbin, R. (2004). GeneWise and genomewise. *Genome Research*, *14*(5), 988–995.

Bolger, A. M., Lohse, M., & Usadel, B. (2014). Trimmomatic: A flexible trimmer for Illumina sequence data. *Bioinformatics*, *30*(15), 2114–2120.

Browning, B. L., & Browning, S. R. (2013). Improving the accuracy and efficiency of identity-by-descent detection in population data. *Genetics*, *194*(2), 459–471.

Browning, B. L., Zhou, Y., & Browning, S. R. (2018). A one-penny imputed genome from next-generation reference panels. *The American Journal of Human Genetics*, *103*(3), 338–348.

Bruce R, K. P. E., Kolovou Brian J, Wilson, & Karim R, Guo S. Q., (2014). ABCB5 is a limbal stem cell gene required for corneal development and repair. *Nature*, *511*(7509), 353–357.

Burge, C., & Karlin, S. (1997). Prediction of complete gene structures in human genomic DNA. *Journal of Molecular Biology*, *268*(1), 78–94.

Caballero, A., Bravo, I., & Wang, J. (2017). Inbreeding load and purging: Implications for the short-term survival and the conservation management of small populations. *Heredity*, *118*(2), 177–185.

Cantarel, B. L., Korf, I., Robb, S. M., Parra, G., Ross, E., Moore, B., & Yandell, M. (2008). MAKER: An easy-to-use annotation pipeline designed for emerging model organism genomes. *Genome Research*, *18*(1), 188–196.

Cho, Y. S., Hu, L., Hou, H., Lee, H., Xu, J., Kwon, S., & Bhak, J. (2013). The tiger genome and comparative analysis with lion and snow leopard genomes. *Nature Communications*, *4*(1), 1–7.

Christie, S. (2010). Why keep tigers in zoos? In R. Tilson & P. J. Nyhus (Eds.), *Tigers of the world* (pp. 205–214). Elsevier.

Cingolani, P., Platts, A., Wang, L. L., Coon, M., Nguyen, T., Wang, L., & Ruden, D. M. (2012). A program for annotating and predicting the effects of single nucleotide polymorphisms, SnpEff: SNPs in the genome of Drosophila melanogaster strain w1118; iso-2; iso-3. *Fly*, *6*(2), 80–92.

Danti, F. R., Galosi, S., Romani, M., Montomoli, M., & Guerrini, R. (2017). GNAO1 encephalopathy: Broadening the phenotype and evaluating treatment and outcome. *Neurology Genetics*, *3*(2), e143.

Danecek, P., Auton, A., Abecasis, G., Albers, C. A., Banks, E., DePristo, M. A., & Sherry, S. T. (2011). The variant call format and VCFtools. *Bioinformatics*, *27*(15), 2156–2158.

DePristo, M. A., Banks, E., Poplin, R., Garimella, K. V., Maguire, J. R., Hartl, C., & Hanna, M. (2011). A framework for variation discovery and genotyping using next-generation DNA sequencing data. *Nature genetics*, *43*(5), 491–498.

Dobrynin, P., Liu, S., Tamazian, G., Xiong, Z., Yurchenko, A. A., Krasheninnikova, K., & O'Brien, S. J. (2015). Genomic legacy of the African cheetah, Acinonyx jubatus. *Genome Biology*, *16*(1), 1–20.

Doherty, K. R., Cave, A., Davis, D. B., & Delmonte, A. J. (2005). Normal myoblast fusion requires myoferlin. *Development*, *132*(24), 5565–5577.

Driscoll, C. A., Yamaguchi, N., Bar-Gal, G. K., Roca, A. L., Luo, S., Macdonald, D. W., & O'Brien, S. J. (2009). Mitochondrial phylogeography illuminates the origin of the extinct Caspian tiger and its relationship to the Amur tiger. *PloS one*, *4*(1), e4125.

Dudchenko, O., Batra, S. S., Omer, A. D., Nyquist, S. K., Hoeger, M., Durand, N. C., & Aiden, A. P. (2017). De novo assembly of the Aedes aegypti genome using Hi-C yields chromosome-length scaffolds. *Science*, *356*(6333), 92–95.

Dumont, B. L., & Payseur, B. A. (2008). Evolution of the genomic rate of recombination in mammals. *Evolution: International Journal of Organic Evolution*, *62*(2), 276–294.

Durand, N. C., Shamim, M. S., Machol, I., Rao, S. S., Huntley, M. H., Lander, E. S., & Aiden, E. L. (2016). Juicer provides a one-click system for analyzing loop-resolution Hi-C experiments. *Cell Systems*, *3*(1), 95–98.

Feng, S. H., Fang, Q., Barnett, R., Li, C., Han, S., Kuhlwilm, M., & Zhang, G. (2019). The genomic footprints of the fall and recovery of the crested ibis. *Current Biology*, *29*(2), 340–349.

Fleming, R. E., & Gitlin, J. (1990). Primary structure of rat ceruloplasmin and analysis of tissue-specific gene expression during development. *Journal of Biological Chemistry*, *265*(13), 7701–7707.

Frankham, R. (1995). Conservation genetics. *Annual Review of Genetics*, *29*(1), 305–327.

Fredrickson, R. J., Siminski, P., Woolf, M., & Hedrick, P. W. (2007). Genetic rescue and inbreeding depression in Mexican wolves. *Proceedings of the Royal Society B: Biological Sciences*, *274*(1623), 2365–2371.

Fujimoto, M., Andrew, M., & Dauber, A. (2020). Disorders caused by genetic defects associated with GH-dependent genes: PAPPA2 defects. *Molecular and Cellular Endocrinology*, *158*(110), 967.

Fujiwara, Y., Ogonuki, N., Inoue, K., Ogura, A., Handel, M. A., Noguchi, J., & Kunieda, T. (2013). t-SNARE Syntaxin2 (STX2) is implicated in intracellular transport of sulfoglycolipids during meiotic prophase in mouse spermatogenesis1. *Biology of Reproduction*, *88*(6), 1–9.

Grantham, R. (1974). Amino acid difference formula to help explain protein evolution. *Science*, *185*(4154), 862–864.

Guang, X. M., Lan, T. M., Wan, Q. H., Huang, Y., Li, H., Zhang, M., & Zhang, L. (2021). Chromosome-scale genomes provide new insights into subspecies divergence and evolutionary characteristics of the giant panda. *Science Bulletin*, *66*(19), 2002–2013.

Gurevich, A., Saveliev, V., Vyahhi, N., & Tesler, G. (2013). QUAST: Quality assessment tool for genome assemblies. *Bioinformatics*, *29*(8), 1072–1075.

Haas, B. J., Salzberg, S. L., Zhu, W., Pertea, M., Allen, J. E., Orvis, J., & Wortman, J. R. (2008). Automated eukaryotic gene structure annotation using EVidenceModeler and the program to assemble spliced alignments. *Genome Biology*, *9*(1), 1–22.

Hasselgren, M., Angerbjörn, A., Eide, N. E., Erlandsson, R., Landa, A., & Norén, K. (2018). Genetic rescue in an inbred Arctic fox (Vulpes lagopus) population. *Proceedings of the Royal Society B: Biological Sciences*, *285*(1875), 20172814.

Hedrick, P. W., & Fredrickson, R. (2010). Genetic rescue guidelines with examples from Mexican wolves and Florida panthers. *Conservation Genetics*, *11*(2), 615–626.

Hohenlohe, P. A., Funk, W. C., & Rajora, O. P. (2021). Population genomics for wildlife conservation and management. *Molecular Ecology*, *30*(1), 62–82.

Huang, X. Y., Hu, D. F., Tang, X. P., Wang, Z. C., & Liu, W. S. (2004). Field survey of south China tigers and their habitat evaluation in Hupingshan National Reserve. *Journal of Zhejiang Agriculture and Forestry University*, *21*(2), 180–184.

Hu, J. Y., Hao, Z. Q., Frantz, L., Wu, S. F., Chen, W., Jiang, Y. F., & Zhang, Y. P. (2020). Genomic consequences of population decline in critically endangered pangolins and their demographic histories. *National Science Review*, *7*(4), 798–814.

Hu, J., Fan, J. P., Sun, Z. Y., & Liu, S. L. (2020). NextPolish: A fast and efficient genome polishing tool for long-read assembly. *Bioinformatics*, *36*(7), 2253–2255.

Ihaka, R., & Gentleman, R. (1996). R: A language for data analysis and graphics. *Journal of Computational and Graphical Statistics*, *5*(3), 299–314.

Jurka, J., Kapitonov, V. V., Pavlicek, A., Klonowski, P., Kohany, O., & Walichiewicz, J. (2005). Repbase Update, a database of eukaryotic repetitive elements. *Cytogenetic and Genome Research*, *110*(1–4), 462–467.

Kai, W., Li, M., & Hakon, H. (2010). ANNOVAR: Functional annotation of genetic variants from high-throughput sequencing data. *Nucleic Acids Research*, *38*(161), e164.

Kanehisa, M., & Goto, S. (2000). KEGG: Kyoto encyclopedia of genes and genomes. *Nucleic Acids Research*, *28*(1), 27–30.

Kardos, M., Akesson, M., Fountain, T., Flagstad, O., Liberg, O., Olason, P., & Ellegren, H. (2018). Genomic consequences of intensive inbreeding in an isolated wolf population. *Nature Ecology & Evolution*, *2*(1), 124–131.

Kelberman, D., Islam, L., Lakowski, J., Bacchelli, C., Chanudet, E., Lescai, F., & Wolf, S. (2014). Mutation of SALL2 causes recessive ocular coloboma in humans and mice. *Human Molecular Genetics*, *23*(10), 2511–2526.

Keller, O., Kollmar, M., Stanke, M., & Waack, S. (2011). A novel hybrid gene prediction method employing protein multiple sequence alignments. *Bioinformatics*, *27*(6), 757–763.

Kendig, K. I., Baheti, S., Bockol, M. A., Drucker, T. M., Hart, S. N., Heldenbrand, J. R., & Klee, E. W. (2019). Sentieon DNASeq variant calling workflow demonstrates strong computational performance and accuracy. *Frontiers in Genetics*, *10*, 736.

Kent, W. J. (2002). BLAT—the BLAST-like alignment tool. *Genome Research*, *12*(4), 656–664.

Khan, A., Patel, K., Shukla, H., Viswanathan, A., van der Valk, T., Borthakur, U., & Kardos, M. (2021). Genomic evidence for inbreeding depression and purging of deleterious genetic variation in Indian tigers. *PNAS*, *118*(49), 1–10.

Kim, H. T., Yin, W., Jin, Y. J., Panza, P., Gunawan, F., Grohmann, B., & Guenther, S. (2018). Myh10 deficiency leads to defective extracellular matrix remodeling and pulmonary disease. *Nature Communications*, *9*(1), 1–13.

Koren, S., Walenz, B. P., Berlin, K., Miller, J. R., Bergman, N. H., & Phillippy, A. M. (2017). Canu: Scalable and accurate long-read assembly via adaptive k-mer weighting and repeat separation. *Genome Research*, *27*(5), 722–736.

Korf, I. (2004). Gene finding in novel genomes. *BMC Bioinformatics*, *5*(1), 1–9.

Kuroki, S., Akiyoshi, M., Tokura, M., Miyachi, H., Nakai, Y., Kimura, H., & Tachibana, M. (2013). JMJD1C, a JmjC domain-containing protein, is required for long-term maintenance of male germ cells in mice. *Biology of Reproduction*, *89*(4), 91–99.

Kusz-Zamelczyk, K., Sajek, M., Spik, A., Glazar, R., Jędrzejczak, P., Latos-Bieleńska, A., & Jaruzelska, J. (2013). Mutations of NANOS1, a human homologue of the Drosophila morphogen, are associated with a lack of germ cells in testes or severe oligo-astheno-teratozoospermia. *Journal of Medical Genetics*, *50*(3), 187–193.

Li, H. (2018). Minimap2: pairwise alignment for nucleotide sequences. *Bioinformatics*, *34*(18), 3094–3100.

Li, H., & Durbin, R. (2010). Fast and accurate long-read alignment with Burrows–Wheeler transform. *Bioinformatics*, *26*(5), 589–595.

Li, H., Handsaker, B., Wysoker, A., Fennell, T., Ruan, J., Homer, N., & Durbin, R. (2009). The sequence alignment/map format and SAMtools. *Bioinformatics*, *25*(16), 2078–2079.

Li, S., Lei, S., & Chen, W. (2013). Preliminary comparation of three feeding methods for South China tiger (*Panthera tigris amoyensis*) cubs. *Acta Theriologica Sinica*, *33*(1), 90–93.

Li, Y., Sha, Y., Wang, X., Ding, L., & Lu, Z. (2019). DNAH2 is a novel candidate gene associated with multiple morphological abnormalities of the sperm flagella (MMAF). *Clinical Genetics*, *95*(5), 590–600.

Lieberman-Aiden, E., Van Berkum, N. L., Williams, L., Imakaev, M., Ragoczy, T., Telling, A., & Dorschner, M. O. (2009). Comprehensive mapping of long-range interactions reveals folding principles of the human genome. *Science*, *326*(5950), 289–293.

Lindner, S. E., Egelston, C. A., Huard, S. M., Lee, P. P., & Wang, L. D. (2020). Arhgap25 deficiency leads to decreased numbers of peripheral blood B cells and defective germinal center reactions. *ImmunoHorizons*, *4*(5), 274–281.

Liu, D., Ma, Y., Li, H., Xu, Y., Zhang, Y., Dahmer, T., & Wang, J. (2013). Simultaneous polyandry and heteropaternity in tiger (Panthera tigris altaica): Implications for conservation of genetic diversity in captive populations of felids. *Chinese Science Bulletin*, *58*(18), 2230–2236.

Liu, Q. X., Wang, A. S., Xia, J. X., He, W., & Zoo, S. (2014). Scent Enrichment to Reduce the Stereotypic Behavior of Captive South China Tiger (*Panthera tigris amoyensis*). *Chinese Journal of Wildlife*., *35*(4), 376–380.

Liu, Y. C., Sun, X., Driscoll, C., Miquelle, D. G., Xu, X., Martelli, P., & Luo, S. J. (2018). Genome-Wide Evolutionary Analysis of Natural History and Adaptation in the World's Tigers. *Current Biology*, *28*(23), 3840–3849.

Luo, S. J., Kim, J. H., Johnson, W. E., Van Der Walt, J., Martenson, J., Yuhki, N., & Quigley, H. B. (2004). Phylogeography and genetic ancestry of tigers (Panthera tigris). *PLoS Biology*, *2*(12), e442.

Luo, S. J., Liu, Y. C., & Xu, X. (2019). Tigers of the world: Genomics and conservation. *Annual Review of Animal Biosciences*, *7*, 521–548.

Ma, J.H, S. W., Xu, W.N, Zhang, X.F, Lu, Q.B. (2020). Study on the individual behavior of captive female south China tigers during parturition. *Chinese Journal of Wildlife*, *41*(3), 746–752.

Majoros, W. H., Pertea, M., & Salzberg, S. L. (2004). TigrScan and GlimmerHMM: Two open source ab initio eukaryotic gene-finders. *Bioinformatics*, *20*(16), 2878–2879.

Manichaikul, A., Mychaleckyj, J. C., Rich, S. S., Daly, K., Sale, M., & Chen, W. M. (2010). Robust relationship inference in genome-wide association studies. *Bioinformatics*, *26*(22), 2867–2873.

Mazák, V. (1983). *Der Tiger: Panthera tigris Linnaeus 1758*. A. Ziemsen.

McQuillan, R., Leutenegger, A. L., Abdel-Rahman, R., Franklin, C. S., Pericic, M., Barac-Lauc, L., & Tenesa, A. (2008). Runs of homozygosity in European populations. *The American Journal of Human Genetics*, *83*(3), 359–372.

Miao, L., Zhu, F., He, B., Ferrat, M., Liu, Q., Cao, X., & Cui, X. (2013). Synthesis of China's land use in the past 300 years. *Global and Planetary Change*, *100*, 224–233.

Mittal, P., Jaiswal, S. K., Vijay, N., Saxena, R., & Sharma, V. K. (2019). Comparative analysis of corrected tiger genome provides clues to its neuronal evolution. *Scientific Reports*, *9*(1), 1–11.

Mount, D. W. (2007). Using the basic local alignment search tool (BLAST). *Cold Spring Harbor Protocols*, *2007*(7), pdb.top17.

Nguyen, L. T., Schmidt, H. A., Von Haeseler, A., & Minh, B. Q. (2015). IQ-TREE: A fast and effective stochastic algorithm for estimating maximum-likelihood phylogenies. *Molecular Biology and Evolution*, *32*(1), 268–274.

Parra, G., Blanco, E., & Guigó, R. (2000). Geneid in drosophila. *Genome Research*, *10*(4), 511–515.

Pittman, D. L., & Schimenti, J. C. (2000). Midgestation lethality in mice deficient for the RecA-related gene, Rad51d/Rad51l3. *Genesis*, *26*(3), 167–173.

Purcell, S., Neale, B., Todd-Brown, K., Thomas, L., Ferreira, M. A., Bender, D., & Daly, M. J. (2007). PLINK: A tool set for whole-genome association and population-based linkage analyses. *The American Journal of Human Genetics*, *81*(3), 559–575.

Rosenberg, N. A., Pemberton, T. J., Li, J. Z., & Belmont, J. W. (2013). Runs of homozygosity and parental relatedness. *Genetics in Medicine*, *15*(9), 753–754.

Saremi, N. F., Supple, M. A., Byrne, A., Cahill, J. A., Coutinho, L. L., Dalén, L., & O'Brien, S. J. (2019). Puma genomes from North and South America provide insights into the genomic consequences of inbreeding. *Nature Communications*, *10*(1), 1–10.

Schiffels, S., & Durbin, R. (2014). Inferring human population size and separation history from multiple genome sequences. *Nat Genetics*, *46*(8), 919–925.

Schiffels, S., & Wang, K. (2020). MSMC and MSMC2: The multiple sequentially markovian coalescent. In *Statistical population genomics* (pp. 147–166). Humana.

Sedlazeck, F. J., Rescheneder, P., Smolka, M., Fang, H., Nattestad, M., Von Haeseler, A., & Schatz, M. C. (2018). Accurate detection of complex structural variations using single-molecule sequencing. *Nature Methods*, *15*(6), 461–468.

Seidensticker, J. (2010). Saving wild tigers: A case study in biodiversity loss and challenges to be met for recovery beyond 2010. *Integrative Zoology*, *5*(4), 285–299.

Seppey, M., Manni, M., & Zdobnov, E. M. (2019). BUSCO: Assessing genome assembly and annotation completeness. *Gene Prediction*, *1962*, 227–245.

Servant, N., Varoquaux, N., Lajoie, B. R., Viara, E., Chen, C. J., Vert, J. P., & Barillot, E. (2015). HiC-Pro: An optimized and flexible pipeline for Hi-C data processing. *Genome Biology*, *16*(1), 1–11.

Shi, J. J., Gao, Q., & Fu, C. Y. Z. (2019). Dennd1a, a susceptibility gene for polycystic ovary syndrome, is essential for mouse embryogenesis. *Developmental Dynamics*, *248*(5), 351–362.

Smit, A., Hubley, R., & Green, P. (2015). RepeatMasker Open-4.0. 2013–2015.

Tarailo-Graovac, M., & Chen, N. (2009). Using RepeatMasker to identify repetitive elements in genomic sequences. *Current Protocols in Bioinformatics*, *25*(1), 4.10. 11–14.10. 14.

Terhorst, J., Kamm, J. A., & Song, Y. S. (2017). Robust and scalable inference of population history from hundreds of unphased whole genomes. *Nature Genetics*, *49*(2), 303–309.

Thompson, E. A. (2013). Identity by descent: Variation in meiosis, across genomes, and in populations. *Genetics*, *194*(2), 301–326.

Tilson, R., Armstrong, D., Miller, E., Byers, A., Traylor-Holzer, K., Brady, G., & Xie, Z. (1996). *Medical, reproductive and management evaluation of south china tigers in China*. Minnesota Zoo.

Tilson, R., Defu, H., Muntifering, J., & Nyhus, P. J. (2004). Dramatic decline of wild South China tigers Panthera tigris amoyensis: Field survey of priority tiger reserves. *Oryx*, *38*(1), 40–47.

Tilson, R., Foose, T., Princee, F., & Traylor-Holzer, K. (1993). *Tiger global animal survival plan*. IUCN/SSC Captive Breeding Specialist Group.

Tilson, R., Traylor-Holzer, K., & Jiang, Q. M. (1997). The decline and impending extinction of the South China tiger. *Oryx*, *31*(4), 243–252.

Wang, B., Harrison, W., Overbeek, P. A., & Zheng, H. (2011). Transposon mutagenesis with coat color genotyping identifies an essential role for Skor2 in sonic hedgehog signaling and cerebellum development. *Development*, *138*(20), 4487.

Wang, Y., Tang, H., DeBarry, J. D., Tan, X., Li, J., Wang, X., & Guo, H. (2012). MCScanX: A toolkit for detection and evolutionary analysis of gene synteny and collinearity. *Nucleic Acids Research*, *40*(7), e49.

Weeks, A. R., Heinze, D., Perrin, L., Stoklosa, J., Hoffmann, A. A., van Rooyen, A., & Mansergh, I. (2017). Genetic rescue increases fitness and aids rapid recovery of an endangered marsupial population. *Nature Communications*, *8*(1), 1–6.

WWF. (2016). The World Wildlife Fund for Nature. https://www.worldwildlife.org/species/tiger

Xu, W.H, L. K., Lin W.M, Chen T.T, Liu D, Fu W.Y.. (2021). Analysis of milk composition of south China tiger (Panthera tigris amoyensis) and development of a tiger milk replacer. *Chinese Journal of Animal Nutrition*, *33*(3), 1724–1734.

Xu, Y. C., Fang, S. G., & Li, Z. K. (2007). Sustainability of the South China tiger: Implications of inbreeding depression and introgression. *Conservation Genetics*, *8*(5), 1199–1207.

Yanai, R., Yamashita, Y., Umezu, K., Hiradate, Y., Hara, K., & Tanemura, K. (2020). Expression and localization of alpha-tubulin N-acetyltransferase 1 in the reproductive system of male mice. *Journal of Reproduction and Development*., *67*(1), 59–66.

Yang, J., Lee, S. H., Goddard, M. E., & Visscher, P. M. (2011). GCTA: A tool for genome-wide complex trait analysis. *American Journal of Human Genetics*, *88*(1), 76–82.

Yang, Q., & He, L. (2017). Spatiotemporal changes in population distribution and socioeconomic development in China from 1950 to 2010. *Arabian Journal of Geosciences*, *10*(22), 498.

Yang, Y., Jiang, C., Zhang, X., Liu, X., Li, J., Qiao, X., & Shen, Y. (2020). Loss-of-function mutation in DNAH8 induces asthenoteratospermia associated with multiple morphological abnormalities of the sperm flagella. *Clinical Genetics*, *98*(4), 396–401.

Yao, H., Goldman, D. C., Nechiporuk, T., Kawane, S., McWeeney, S. K., Tyner, J. W., & Fleming, W. H. (2014). Corepressor Rcor1 is essential for murine erythropoiesis. *Blood, The Journal of the American Society of Hematology*, *123*(20), 3175–3184.

Yoshida, G. M., Cáceres, P., Marín-Nahuelpi, R., Koop, B. F., & Yáñez, J. M. (2020). Estimates of autozygosity through runs of homozygosity in farmed coho salmon. *Genes*, *11*(5), 490.

Yuan, Y. H., Pei, E. L., & Liu, Q. X. (2020). Reproductive parameters of female South China Tigers in captivity. *European Journal of Wildlife Research*, *66*(3), 1–6.

Yuan, Y. H., Yin, Y. Z., & Liu, Q. X. (2021). Inbreeding depression and population viability analysis of the South China tigers (*Panthera tigris amoyensis*) in captivity. *Mammalian Biology*, *4*, 1–7.

Zhang, W. P., Xu, X., Yue, B. S., Hou, R., Xie, J., Zou, Z. T., & Zhang, Z. (2019). Sorting out the genetic background of the last surviving south China tigers. *Journal of Heredity*, *110*(6), 641–650.

SUPPORTING INFORMATION

Additional supporting information can be found online in the Supporting Information section at the end of this article.

How to cite this article: Zhang, L., Lan, T., Lin, C., Fu, W., Yuan, Y., Lin, K., Li, H., Sahu, S. K., Liu, Z., Chen, D., Liu, Q., Wang, A., Wang, X., Ma, Y., Li, S., Zhu, Y., Wang, X., Ren, X., Lu, H. … Xu, Y. (2023). Chromosome-scale genomes reveal genomic consequences of inbreeding in the South China tiger: A comparative study with the Amur tiger. *Molecular Ecology Resources*, *23*, 330–347. https://doi.org/10.1111/1755-0998.13669